

Supplementary Information

Understanding the Second & Third Order Nonlinear Optical Responses of M@b₆₄/b₆₆Al₁₂N₁₂ nanoparticles: A Comprehensive DFT and TD-DFT Study

Meriem Zaidi^{a,b}, Douniazed Hannachi*^{c, d}, Nahla Chaoui^a, Henry Chermette*^e

^a. Département de Chimie, Faculté des Sciences, Université Ferhat Abbas, Setif-1, Algérie.

^b. Laboratoire de Chimie, Ingénierie Moléculaire et Nanostructures (LCIMN), Université Ferhat Abbas Sétif 1, Sétif 19000, Algeria.

^c. Laboratoire d'Électrochimie, d'Ingénierie Moléculaire et de Catalyse Redox (LEIMCR), Département d'Enseignement de Base en Technologie, Faculté de Technologie, Université Ferhat Abbas, Sétif-1, Algérie.

^d. Département de Chimie, Faculté des Sciences de la Matière, Université de Batna-1, Algérie

^e. Université de Lyon, Université Claude Bernard Lyon 1, Institut des Sciences Analytiques, UMR CNRS 5280, 69622 Villeurbanne Cedex, France

Table of contents

Table S1. Delocalization Indices ($\delta(M, A)$ where A= N or Al and M: from Sc to Zn) for $M@b_{64}Al_{12}N_{12}$ and $M@b_{66}Al_{12}N_{12}$	S3
Table S2a. Excitation energy ($E_{0 \rightarrow n}$, eV) and wavelength ($\lambda_{0 \rightarrow n}$, nm), oscillator strengths ($f_{0 \rightarrow n}$, dimensionless), Integral of hole and electron, transition dipole moment ($\Delta\mu_{0 \rightarrow n}$, A.u.), S_m index, $S_r(r)$ overlap, charge transfer distance (D index, Å), RMSD of hole and electron (Å), H and t indexes (Å), the hole delocalization index (HDI) and electron delocalization index (EDI)associated to the $S_0 \rightarrow S_n$ transition, as calculated at the cam-b3lyp/6-311+g(d) of the studied compounds $M@b_{64}Al_{12}N_{12}$	S4
Table S2b. Excitation energy ($E_{0 \rightarrow n}$, eV) and wavelength ($\lambda_{0 \rightarrow n}$, nm), oscillator strengths ($f_{0 \rightarrow n}$, dimensionless), Integral of hole and electron, transition dipole moment ($\Delta\mu_{0 \rightarrow n}$, A.u.), S_m index, $S_r(r)$ overlap, charge transfer distance (D index, Å), RMSD of hole and electron (Å), H and t indexes (Å), the hole delocalization index (HDI) and electron delocalization index (EDI)associated to the $S_0 \rightarrow S_n$ transition, as calculated at the cam-b3lyp/6-311+g(d) of the studied compounds $M@b_{66}Al_{12}N_{12}$	S6
Table S3. Static and dynamic of $\beta_{J=1}$ and $\beta_{J=3}$ of $M@b_{64/66}Al_{12}N_{12}$ (M= Sc to Zn)	S9
Table S4. The frequency dispersion factor (FDF^λ) between static and dynamic HRS hyperpolarizability at a specific wavelength ($\lambda=1064, 1341$ and 1906 nm)	S10
Table S5. Static and dynamic second hyperpolarizability (au) for $Al_{12}N_{12}$	S10
Table S6. Static and dynamic first hyperpolarizability (au) and depolarization ratio (DR) for $M@b_{64/66}Al_{12}N_{12}$ (M= Sc- Zn) calculated by the sum-over-states method	S11
Scheme S1. Optimized geometry of the title compound	S12
Figure S1. Molecular topology of $M@b_{64/66}Al_{12}N_{12}$ (M= Sc- Zn)	S13
Figure S2. Calculated UV – vis absorption spectra of $M@b_{64/66}Al_{12}N_{12}$ (M from Sr to Zn)	S18
Figure S3. Molecular orbitals (MO) and electron density difference maps (EDDM) for the crucial excited states of $M@b_{64}Al_{12}N_{12}$ and $M@b_{66}Al_{12}N_{12}$	S31
Figure S4. Variation of first hyperpolarizability (β_{HRS}^∞) and second hyperpolarizability ($\gamma(0;0,0,0)$) of $M@b_{64}Al_{12}N_{12}$ (red) and $M@b_{66}Al_{12}N_{12}$ (blue) where M= Sc-Zn	S32
Figure S5. Relationship between $I_{\Psi V}^{2w}$ and polarization angle Ψ of $M@b_{64/66}Al_{12}N_{12}$	S33
Figure S6. Plot of β_{HRS}^λ as a function of β_{SHG}^λ for $M@b_{64/66}Al_{12}N_{12}$, where M= Sc to Zn), 1906, 1341, and 1064 nm	S34

Table S1. Delocalization Indices ($\delta(M, A)$ where A= N or Al and M: from Sc to Zn) for M@b₆₄Al₁₂N₁₂ and M@b₆₆Al₁₂N₁₂

M@b ₆₄ Al ₁₂ N ₁₂	Sc	Ti	V	Cr	Mn	Fe	Co	Ni	Cu	Zn	M@b ₆₆ Al ₁₂ N ₁₂	Sc	Ti	V	Cr	Mn	Fe	Co	Ni	Cu	Zn
1(AL)	0.93	0.94	0.95	0.81	0.72	0.81	0.81	0.82	0.77	0.65	1(AL)	0.01	0.01	0.01	0.01	0.009	0.009	0.009	0.008	0.009	0.007
2(AL)	0.27	0.27	0.23	0.18	0.15	0.16	0.15	0.14	0.15	0.11	2(AL)	0.005	0.004	0.003	0.003	0.003	0.002	0.002	0.002	0.002	0.002
3(N)	1.74	1.74	1.65	1.29	1.14	1.17	1.12	1.08	1.20	0.80	3(N)	0.002	0.002	0.001	0.001	0.001	0.001	0.001	0.001	0.001	0.001
4(N)	0.11	0.11	0.09	0.06	0.06	0.06	0.05	0.05	0.06	0.05	4(N)	0.01	0.01	0.01	0.009	0.008	0.008	0.007	0.007	0.008	0.005
5(AL)	0.01	0.01	0.01	0.01	0.009	0.009	0.01	0.009	0.01	0.007	5(AL)	0.02	0.01	0.01	0.01	0.01	0.01	0.01	0.01	0.01	0.01
6(AL)	0.01	0.01	0.01	0.008	0.008	0.009	0.008	0.008	0.009	0.007	6(AL)	0.90	0.87	0.86	0.84	0.74	0.85	0.83	0.83	0.79	0.66
7(N)	0.06	0.06	0.06	0.04	0.04	0.04	0.04	0.04	0.04	0.04	7(N)	0.04	0.04	0.04	0.03	0.03	0.03	0.03	0.03	0.03	0.03
8(N)	0.003	0.003	0.003	0.002	0.002	0.003	0.002	0.002	0.002	0.002	8(N)	0.04	0.04	0.04	0.03	0.03	0.03	0.03	0.03	0.03	0.03
9(AL)	0.0008	0.0007	0.0006	0.0005	0.0006	0.0006	0.0005	0.0004	0.0004	0.0004	9(AL)	0.005	0.004	0.003	0.003	0.003	0.002	0.002	0.002	0.002	0.002
10(AL)	0.002	0.002	0.002	0.002	0.002	0.002	0.001	0.001	0.001	0.001	10(AL)	0.01	0.01	0.01	0.01	0.009	0.009	0.009	0.008	0.009	0.007
11(N)	0.001	0.001	0.001	0.0007	0.0007	0.0006	0.0005	0.0005	0.0005	0.0004	11(N)	0.002	0.002	0.001	0.001	0.001	0.001	0.001	0.001	0.001	0.001
12(N)	0.0002	0.0002	0.0002	0.0002	0.0002	0.0002	0.0001	0.0001	0.0001	0.0001	12(N)	0.01	0.01	0.01	0.009	0.008	0.008	0.007	0.007	0.008	0.005
13(AL)	0.005	0.004	0.004	0.003	0.004	0.004	0.003	0.003	0.004	0.003	13(AL)	0.001	0.0009	0.0007	0.0006	0.0006	0.0005	0.0005	0.0004	0.0004	0.0003
14(AL)	0.004	0.003	0.003	0.003	0.003	0.003	0.003	0.003	0.003	0.003	14(AL)	0.01	0.009	0.008	0.007	0.008	0.008	0.007	0.007	0.007	0.007
15(N)	0.0008	0.0008	0.0006	0.0006	0.0006	0.0005	0.0005	0.0004	0.0004	0.0003	15(N)	0.001	0.0009	0.0007	0.0006	0.0006	0.0006	0.0005	0.0005	0.0005	0.0004
16(N)	0.01	0.01	0.011	0.009	0.01	0.01	0.009	0.008	0.009	0.008	16(N)	0.001	0.0009	0.0007	0.0006	0.0006	0.0006	0.0005	0.0005	0.0005	0.0004
17(AL)	0.02	0.02	0.02	0.01	0.01	0.01	0.01	0.01	0.01	0.01	17(AL)	0.23	0.21	0.19	0.16	0.01	0.14	0.13	0.12	0.13	0.08
18(AL)	0.001	0.001	0.001	0.001	0.001	0.001	0.001	0.001	0.001	0.001	18(AL)	0.24	0.22	0.19	0.17	0.14	0.14	0.13	0.12	0.13	0.08
19(N)	0.001	0.001	0.001	0.001	0.001	0.001	0.001	0.001	0.001	0.001	19(N)	1.58	1.46	1.41	1.28	1.14	1.18	1.12	1.10	1.19	0.80
20(N)	0.002	0.002	0.002	0.002	0.002	0.002	0.001	0.001	0.001	0.001	20(N)	0.03	0.02	0.02	0.02	0.02	0.02	0.01	0.01	0.02	0.01
21(AL)	0.29	0.28	0.26	0.20	0.17	0.16	0.16	0.14	0.16	0.11	21(AL)	0.002	0.002	0.001	0.001	0.001	0.001	0.001	0.001	0.001	0.001
22(AL)	0.008	0.008	0.007	0.005	0.005	0.004	0.004	0.004	0.004	0.004	22(AL)	0.002	0.002	0.001	0.001	0.001	0.001	0.001	0.001	0.001	0.001
23(N)	0.031	0.02	0.02	0.01	0.01	0.009	0.009	0.008	0.01	0.005	23(N)	0.003	0.003	0.003	0.002	0.002	0.002	0.002	0.002	0.002	0.002
24(N)	0.01	0.01	0.01	0.009	0.009	0.009	0.008	0.008	0.008	0.008	24(N)	0.0003	0.0003	0.0002	0.0002	0.0002	0.0002	0.0001	0.0001	0.0001	0.0001

25(M)	3.55	3.55	3.40	2.69	2.39	2.52	2.45	2.38	2.50	1.85	25(M)	3.21	3.01	2.86	2.65	2.34	2.50	2.39	2.35	2.42	1.79
-------	------	------	------	------	------	------	------	------	------	------	-------	------	------	------	------	------	------	------	------	------	------

Table S2a. Excitation energy ($E_{0 \rightarrow n}$, eV) and wavelength ($\lambda_{0 \rightarrow n}$, nm), oscillator strengths ($f_{0 \rightarrow n}$, dimensionless), Integral of hole and electron, transition dipole moment ($\Delta\mu_{0 \rightarrow n}$, a.u), S_m index, $S_r(r)$ overlap, charge transfer distance (D index, Å), RMSD of hole and electron (Å), H and t indexes (Å), the hole delocalization index (HDI) and electron delocalization index (EDI) associated to the $S_0 \rightarrow S_n$ transition, as calculated at the cam-b3lyp/6-311+g(d) of the studied compounds $M@b_{64}Al_{12}N_{12}$

	$S_{0 \rightarrow n}$	$\Delta E_{0 \rightarrow n}$	$\Delta\lambda_{0 \rightarrow n}$	$f_{0 \rightarrow n}$	Integral of hole	Integral of electron	$\Delta\mu_{0 \rightarrow n}$	S_m	S_r	D index	RMSD hole	RMSD electron	H_{index}	t_{index}	HDI	EDI
$Sc@b_{64}Al_{12}N_{12}$	$S_{0 \rightarrow 5}$	1.617	766.853	0.009	0.999	0.988	2.037	0.499	0.795	1.085	2.210	2.607	2.408	-0.434		
	$S_{0 \rightarrow 11}$	2.478	500.262	0.01	0.997	0.986	3.399	0.398	0.690	1.813	2.196	3.711	2.953	-0.095	8.77	4.39
	$S_{0 \rightarrow 13}$	2.676	463.235	0.144	0.999	0.964	2.201	0.278	0.578	1.187	2.368	3.284	2.826	-0.443	6.94	7.12
	$S_{0 \rightarrow 15}$	2.925	423.836	0.121	0.999	0.986	1.952	0.377	0.667	1.04	2.379	2.456	2.418	-0.534	6.87	10.08
$Ti@b_{64}Al_{12}N_{12}$	$S_{0 \rightarrow 5}$	1.245	996.102	0.005	0.999	0.986	1.177	0.305	0.597	0.628	1.481	2.030	1.755	-0.455	20.22	13.05
	$S_{0 \rightarrow 15}$	2.886	429.638	0.022	0.998	0.987	4.024	0.282	0.589	2.144	2.115	3.814	2.964	0.237	11.54	3.73
	$S_{0 \rightarrow 18}$	3.151	393.528	0.126	0.999	0.988	1.178	0.425	0.732	0.628	2.163	2.597	2.38	-0.796	10.72	8.07
	$S_{0 \rightarrow 16}$	2.895	428.302	0.055	0.999	0.983	1.441	0.366	0.662	1.044	2.252	3.693	2.972	-0.749	7.91	4.34
$V@b_{64}Al_{12}N_{12}$	$S_{0 \rightarrow 5}$	1.508	822.454	0.001	0.999	0.993	0.831	0.292	0.596	0.442	1.327	1.984	1.655	-0.588	25.90	15.88
	$S_{0 \rightarrow 14}$	2.985	415.346	0.057	0.999	0.984	2.59	0.286	0.579	1.381	2.302	3.913	3.107	-0.602	7.84	3.76
	$S_{0 \rightarrow 15}$	3.041	407.751	0.116	0.999	0.979	1.675	0.453	0.757	0.896	2.250	2.742	2.496	-0.773	8.61	7.87
	$S_{0 \rightarrow 17}$	3.358	369.211	0.024	1.000	0.987	2.82	0.329	0.628	1.502	2.207	3.692	2.949	-0.329	12.52	4.12
$Cr@b_{64}Al$	$S_{0 \rightarrow 1}$	1.352	917.319	0.001	0.999	0.990	1.048	0.321	0.602	0.558	1.460	2.115	1.788	-0.736	29.66	14.99
	$S_{0 \rightarrow 7}$	2.558	484.695	0.088	0.998	0.980	2.267	0.285	0.590	1.213	2.305	3.931	3.118	-0.664	7.31	3.7
	$S_{0 \rightarrow 11}$	3.08	402.588	0.110	0.999	0.986	0.629	0.353	0.669	0.335	1.814	2.977	2.396	-1.147	19.82	5.23

	$S_{0 \rightarrow 16}$	3.508	353.465	0.054	0.999	0.981	1.512	0.456	0.759	0.808	2.349	3.547	2.948	-0.935	9.9	7.96
$\text{Mn}@b_{64}\text{Al}_{12}\text{N}$	$S_{0 \rightarrow 1}$	1.458	850.610	0.01	0.997	0.993	0.46	0.603	0.86	0.245	2.223	2.487	2.355	-1.195	6.73	6.34
	$S_{0 \rightarrow 6}$	2.563	483.730	0.043	0.996	0.993	3.736	0.322	0.631	1.987	2.319	3.543	2.931	0.020	6.64	8.82
	$S_{0 \rightarrow 8}$	2.928	423.402	0.073	0.999	0.987	1.525	0.41	0.715	0.813	2.301	3.456	2.878	-1.067	8.85	14.91
	$S_{0 \rightarrow 9}$	2.98	416.112	0.140	0.999	0.98	2.254	0.414	0.733	1.205	2.289	2.795	2.542	-0.443	8.8	8.75
	$S_{0 \rightarrow 4}$	1.301	952.704	0.023	0.997	0.993	0.309	0.603	0.872	0.164	2.126	2.286	2.206	-1.171	9.6	11.55
$\text{Fe}@b_{64}\text{Al}_{12}\text{N}_{12}$	$S_{0 \rightarrow 9}$	2.42	512.334	0.057	0.996	0.991	5.929	0.187	0.486	3.156	2.348	3.891	3.12	1.111	7.88	3.11
	$S_{0 \rightarrow 13}$	3.17	391.119	0.085	0.999	0.980	1.568	0.421	0.727	0.839	2.104	2.913	2.508	-0.842	14.84	7.7
	$S_{0 \rightarrow 15}$	3.538	350.467	0.022	0.999	0.989	4.551	0.2	0.465	2.421	2.56	3.944	3.252	0.279	13.44	2.92
	$S_{0 \rightarrow 8}$	1.728	717.713	<0.001	1.000	0.996	0.620	0.293	0.581	0.329	1.565	1.394	1.479	-0.633	27.88	36.89
	$S_{0 \rightarrow 9}$	1.848	671.059	0.072	0.997	0.988	0.672	0.512	0.805	0.358	2.179	2.573	2.376	-1.001	8.77	6.24
$\text{Co}@b_{64}\text{Al}_{12}\text{N}_1$	$S_{0 \rightarrow 11}$	2.545	487.113	0.064	0.997	0.991	6.270	0.158	0.435	3.336	2.342	3.901	3.121	1.325	7.55	2.98
	$S_{0 \rightarrow 13}$	3.062	404.862	0.008	1.001	0.987	0.124	0.18	0.45	0.066	1.244	2.563	1.903	-1.186	38.63	6.19
	$S_{0 \rightarrow 5}$	1.833	676.220	0.037	0.998	0.989	0.306	0.594	0.845	0.163	1.963	2.461	2.212	-1.305	18.65	8.03
	$S_{0 \rightarrow 7}$	2.582	480.152	0.055	0.997	0.991	5.838	0.175	0.469	3.107	2.35	3.884	3.117	1.098	8.29	2.99
	$S_{0 \rightarrow 13}$	3.657	339.007	0.002	0.999	0.987	1.209	0.225	0.519	0.644	3.035	4.007	3.521	-1.244	9.55	4.70
$\text{Ni}@b_{64}\text{Al}_{12}\text{N}_{12}$	$S_{0 \rightarrow 14}$	3.755	330.221	<0.001	0.999	0.986	0.764	0.271	0.562	0.407	3.499	4.082	3.79	-1.782	7.33	2.62
	$S_{0 \rightarrow 1}$	2.095	591.955	0.076	0.998	0.984	1.25	0.445	0.726	0.667	2.175	2.54	2.357	-0.782	11.00	5.77
	$S_{0 \rightarrow 2}$	2.647	468.362	0.057	0.998	0.99	5.548	0.194	0.489	2.952	2.328	3.930	3.129	0.927	9.12	2.89
	$S_{0 \rightarrow 9}$	3.61	343.448	0.001	0.999	0.988	0.817	0.277	0.586	0.435	3.072	3.916	3.494	-1.369	10.80	4.56
	$S_{0 \rightarrow 11}$	3.745	331.041	<0.001	0.999	0.988	0.362	0.209	0.501	0.193	3.264	4.015	3.639	-1.765	8.63	2.71
$\text{Cu}@b_{64}\text{Al}_{12}\text{N}_1$	$S_{0 \rightarrow 3}$	2.994	414.111	0.215	0.999	0.990	0.412	0.409	0.699	0.219	2.286	2.649	2.468	-1.546	9.10	6.09
	$S_{0 \rightarrow 5}$	3.332	372.070	0.09	0.999	0.992	5.752	0.153	0.413	3.057	2.425	3.887	3.156	1.006	8.24	3.03
	$S_{0 \rightarrow 8}$	3.863	320.922	0.085	0.999	0.993	1.449	0.329	0.598	0.770	2.496	3.28	2.888	-0.699	8.04	3.66
	$S_{0 \rightarrow 11}$	3.977	311.723	0.002	0.999	0.987	0.671	0.233	0.514	0.357	3.289	4.085	3.687	-1.748	8.36	2.49

Table S2b. Excitation energy ($E_{0 \rightarrow n}$, eV) and wavelength ($\lambda_{0 \rightarrow n}$, nm), oscillator strengths ($f_{0 \rightarrow n}$, dimensionless), Integral of hole and electron, transition dipole moment ($\Delta\mu_{0 \rightarrow n}$, A.u.), S_m index, $S_r(r)$ overlap, charge transfer distance (D index, Å), RMSD of hole and electron (Å), H and t indexes (Å), the hole delocalization index (HDI) and electron delocalization index (EDI) associated to the $S_0 \rightarrow S_n$ transition, as calculated at the cam-b3lyp/6-311+g(d) of the studied compounds $M@b_{66}Al_{12}N_{12}$

	$S_{0 \rightarrow n}$	$E_{0 \rightarrow n}$	$\lambda_{0 \rightarrow n}$	$f_{0 \rightarrow n}$	Integral of hole	electron	$\Delta\mu_{0 \rightarrow n}$	S_m	Sr	D index	RMSD hole	RMSD electron	H index	t index	HDI	EDI
$Sc@b_{66}Al_{12}N_{12}$	$S_{0 \rightarrow 6}$	1.401	885.227	0.001	0.997	0.996	0.982	0.398	0.706	0.522	1.882	2.268	2.084	-0.710	11.90	9.94
	$S_{0 \rightarrow 10}$	2.095	591.898	0.013	0.998	0.990	3.866	0.387	0.702	2.058	2.012	3.617	2.814	0.238	10.98	4.55
	$S_{0 \rightarrow 13}$	2.350	527.618	0.251	0.998	0.957	1.888	0.348	0.658	1.022	2.413	3.045	2.729	-0.739	6.24	6.04
	$S_{0 \rightarrow 24}$	3.482	356.125	0.121	0.998	0.989	2.618	0.354	0.641	1.394	2.413	3.224	2.818	-0.141	6.14	4.78
$Ti@b_{66}Al_{12}N_{12}$	$S_{0 \rightarrow 8}$	1.480	837.905	<0.001	0.999	0.996	0.247	0.521	0.802	0.131	1.927	2.277	2.102	-1.166	11.43	9.98
	$S_{0 \rightarrow 13}$	2.100	590.264	0.177	0.998	0.975	1.590	0.356	0.670	0.853	2.310	2.942	2.626	-0.837	7.16	7.15
	$S_{0 \rightarrow 15}$	2.330	532.192	<0.001	0.998	0.991	3.371	0.368	0.667	1.793	2.380	3.689	3.034	-0.229	6.62	6.69
	$S_{0 \rightarrow 16}$	2.392	518.310	0.01	0.999	0.993	3.392	0.343	0.640	1.802	1.684	3.427	2.556	0.187	15.77	4.92
$V@b_{66}Al_{12}N_{12}$	$S_{0 \rightarrow 7}$	1.443	859.34	<0.001	0.999	0.990	0.966	0.256	0.544	0.514	1.078	1.749	1.414	-0.455	28.06	16.45
	$S_{0 \rightarrow 8}$	1.830	677.550	0.003	0.998	0.991	1.382	0.570	0.847	0.735	2.157	2.488	2.322	-0.691	8.06	7.41
	$S_{0 \rightarrow 12}$	2.503	495.325	0.075	0.999	0.991	3.033	0.309	0.594	1.841	2.297	3.770	3.033	-0.195	7.33	7.50
	$S_{0 \rightarrow 16}$	2.834	437.552	0.059	0.998	0.984	2.476	0.340	0.652	1.321	2.139	3.361	2.750	-0.308	8.60	9.12
$Cr@b_{66}Al_{12}N_{12}$	$S_{0 \rightarrow 1}$	1.439	861.664	<0.001	0.999	0.991	1.008	0.318	0.601	0.536	1.383	2.022	1.702	-0.723	30.24	15.24
	$S_{0 \rightarrow 7}$	2.504	495.127	0.097	0.999	0.981	2.636	0.278	0.579	1.409	2.272	3.890	3.081	-0.411	7.46	3.61
	$S_{0 \rightarrow 11}$	3.072	403.610	0.006	0.999	0.994	2.829	0.422	0.737	1.502	2.203	2.816	2.510	0.118	8.69	7.10
	$S_{0 \rightarrow 16}$	3.473	356.976	0.061	0.999	0.987	4.548	0.277	0.582	2.423	2.313	3.868	3.089	0.367	11.94	3.34
M	$S_{0 \rightarrow 1}$	1.466	845.563	0.011	0.995	0.995	0.624	0.594	0.858	0.332	2.195	2.478	2.336	-1.199	6.72	6.23

	$S_{0 \rightarrow 4}$	2.354	526.699	0.024	0.994	0.992	4.788	0.269	0.566	2.550	2.297	3.631	2.964	0.560	6.85	5.59
	$S_{0 \rightarrow 8}$	2.924	424.054	0.118	0.998	0.990	1.901	0.469	0.771	1.011	2.230	2.874	2.552	-0.542	9.51	8.10
n	$S_{0 \rightarrow 9}$	2.990	414.665	0.085	0.998	0.989	4.717	0.289	0.561	2.512	2.318	3.905	3.112	0.416	8.82	7.14
	$S_{0 \rightarrow 4}$	1.431	866.119	0.022	0.997	0.995	0.400	0.576	0.848	0.213	2.082	2.299	2.191	-1.111	8.64	9.01
	$S_{0 \rightarrow 9}$	2.416	513.182	0.05	0.996	0.991	6.208	0.157	0.439	3.305	2.304	3.761	3.032	1.354	7.60	3.24
	$S_{0 \rightarrow 13}$	3.244	382.162	0.129	0.999	0.985	1.181	0.435	0.723	0.630	2.092	3.139	2.615	-0.852	14.39	6.42
	$S_{0 \rightarrow 14}$	3.143	356.555	0.037	0.999	0.989	5.005	0.194	0.445	2.663	2.387	3.899	3.143	0.608	13.28	2.97
	$S_{0 \rightarrow 7}$	1.542	804.000	0.031	0.998	0.993	0.252	0.587	0.856	0.134	1.926	2.367	2.147	-1.170	15.37	8.94
	$S_{0 \rightarrow 9}$	2.428	510.604	0.049	0.997	0.991	6.040	0.158	0.438	3.214	2.307	3.770	3.039	1.260	8.13	3.28
	$S_{0 \rightarrow 13}$	3.284	377.508	0.088	0.999	0.986	0.815	0.374	0.659	0.435	1.865	3.010	2.437	-0.962	22.13	5.36
	$S_{0 \rightarrow 18}$	3.769	328.968	0.022	1.000	0.988	2.971	0.226	0.506	1.582	3.510	4.075	3.792	-1.001	11.58	2.62
	$S_{0 \rightarrow 5}$	1.909	649.646	0.068	0.997	0.989	0.750	0.501	0.803	0.400	2.101	2.501	2.301	-0.940	10.00	6.09
	$S_{0 \rightarrow 7}$	2.479	500.221	0.056	0.997	0.991	5.983	0.161	0.444	3.184	2.301	3.818	3.060	1.221	8.35	3.12
	$S_{0 \rightarrow 14}$	3.685	336.467	<0.001	0.999	0.990	1.219	0.202	0.485	0.648	2.982	3.925	3.454	-1.345	10.55	3.63
	$S_{0 \rightarrow 16}$	3.843	322.642	0.001	0.999	0.987	1.024	0.240	0.523	0.546	2.848	3.857	3.353	-1.413	10.75	2.88
	$S_{0 \rightarrow 1}$	1.993	622.195	0.077	0.997	0.987	1.293	0.437	0.711	0.689	2.120	2.476	2.298	-0.701	11.12	5.97
	$S_{0 \rightarrow 2}$	2.521	491.847	0.053	0.997	0.991	5.799	0.158	0.424	3.085	2.295	3.836	3.065	1.128	9.29	3.14
	$S_{0 \rightarrow 9}$	3.609	343.525	<0.001	0.999	0.991	1.435	0.235	0.533	0.763	2.800	3.800	3.300	-1.040	11.07	4.60
	$S_{0 \rightarrow 12}$	3.776	328.385	<0.001	0.999	0.989	0.629	0.215	0.508	0.335	3.256	3.995	3.625	-1.638	8.29	2.63
	$S_{0 \rightarrow 3}$	2.901	427.416	0.197	0.999	0.992	0.439	0.404	0.694	0.233	2.286	2.581	2.434	-1.505	9.41	6.12
	$S_{0 \rightarrow 5}$	3.198	387.695	0.076	0.999	0.993	5.527	0.137	0.386	2.936	2.448	3.769	3.108	0.940	8.66	3.25
	$S_{0 \rightarrow 11}$	3.975	311.888	0.02	0.999	0.990	0.555	0.245	0.525	0.296	3.428	4.195	3.812	-1.776	8.26	2.35
	$S_{0 \rightarrow 15}$	4.076	304.190	0.002	0.999	0.990	1.240	0.229	0.506	0.660	2.704	3.807	3.255	-1.252	11.14	2.93

Table S3. Static and dynamic of $\beta_{J=1}$ and $\beta_{J=3}$ of $M@b_{64/66}Al_{12}N_{12}$ (M= Sc to Zn)

	M@b₆₄Al₁₂N₁₂	Sc	Ti	V	Cr	Mn	Fe	Co	Ni	Cu	Zn
$\lambda=\infty$	$\beta_{J=1}$	14082.173	5891.150	3560.841	4142.269	1292.168	1374.754	1640.612	1777.973	1948.246	860.349
	$\beta_{J=3}$	5119.968	1993.380	1179.743	1696.278	1519.675	1589.217	1309.425	1253.303	1360.834	620.968
$\lambda=1064$	$\beta_{J=1}$	/	/	6318.396	7379.356	12029.27	22404.68	/	7024.467	11448.645	1956.270
	$\beta_{J=3}$	800942.12	23387.25	20807.15	3471.322	22583.75	61527.43	25976.228	13889.98	16006.481	2150.988
$\lambda=1341$	$\beta_{J=1}$	/	36131.39	9285.109	25843.95	4731.52	/	86633.456	29896.341	9180.305	1372.268
	$\beta_{J=3}$	816418.85	32861.10	12613.71	42822.67	5067.94	8296.31	118686.56	48219.500	8795.594	1208.057
$\lambda=1906$	$\beta_{J=1}$	18301.438	428459.85	4600.096	6918.910	5148.929	/	2721.066	2900.709	3226.935	1125.387

$\beta_{J=3}$	34813.893	794286.71	3096.453	2242.221	5137.823	32898.960	2344.314	2642.910	2523.836	848.388	
M@ $b_{66}Al_{12}N_{12}$	Sc	Ti	V	Cr	Mn	Fe	Co	Ni	Cu	Zn	
$\lambda=\infty$	$\beta_{J=1}$	12125.018	9280.389	5533.168	4197.558	1319.535	1188.119	4197.558	1488.229	1979.818	842.727
	$\beta_{J=3}$	4145.306	4093.373	2276.701	1631.493	1368.097	1219.031	1631.493	1004.836	1268.424	516.981
$\lambda=1064$	$\beta_{J=1}$	1137438.70	81721.71	38578.18	7862.451	91739.242	25656.773	7862.451	13567.942	12388.328	2010.291
	$\beta_{J=3}$	4715675.00	131175.95	32515.08	8331.589	152580.42	55179.804	8331.589	24315.702	19872.785	2182.833
$\lambda=1341$	$\beta_{J=1}$	4841922.84	47146.105	15101.44	21294.39	3805.077	1193.521	21294.394	23943.400	15885.973	1350.866
	$\beta_{J=3}$	3948308.13	143268.74	28285.74	44212.05	6309.325	7677.550	44212.058	33586.982	16323.787	1077.724
$\lambda=1906$	$\beta_{J=1}$	/	8551.052	2817.618	6892.510	5221.953	83629.240	2496.547	2457.599	3547.729	1100.944
	$\beta_{J=3}$	17685.454	4336.656	3333.323	3454.442	4956.441	65608.133	2993.989	2105.365	2713.623	718.640

Table S4. The frequency dispersion factor (FDF^λ) between static and dynamic HRS hyperpolarizability at a specific wavelength ($\lambda=1064$, 1341 and 1906 nm)

M@ $b_{66}Al_{12}N_{12}$	Sc	Ti	V	Cr	Mn	Fe	Co	Ni	Cu	Zn
FDF^{1064}	34.6664845	2.50648812	4.12105122	1.80046299	11.6878049	26.7342996	7.10155856	5.86796377	7.24475428	2.53310594
FDF^{1341}	27.1856166	6.96903773	3.41029855	8.8909197	3.54362276	2.73763412	62.8675877	22.2032457	5.05852634	1.66451311
FDF^{1906}	2.01924192	111.662467	1.37965208	1.64926272	3.77133919	10.4290727	1.68769196	1.72485592	1.69229307	1.31889156
M@ $b_{66}Al_{12}N_{12}$	Sc	Ti	V	Cr	Mn	Fe	Co	Ni	Cu	Zn
FDF^{1064}	264.789643	12.2723311	7.68900761	2.20928456	85.0416993	30.9573248	25.5779815	12.8545885	8.36765175	2.7158968
FDF^{1341}	441.742669	10.8674289	4.1697784	8.29611044	3.52146153	3.60934547	3.23285776	19.978546	8.91788538	1.6781584
FDF^{1906}	0.80945292	0.93275904	0.62191629	1.67478826	3.85503873	65.6862151	2.42172551	1.73170134	1.8480803	1.3183448

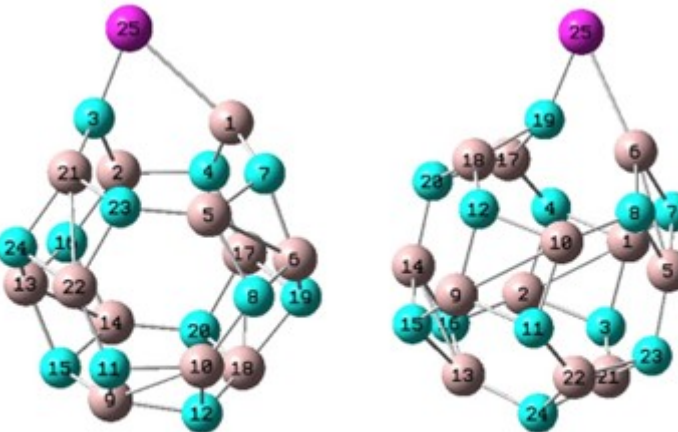
Table S5. Static and dynamic second hyperpolarizability (au) for $^{Al_{12}N_{12}}$

$\gamma(0;0,0,0)$	$\lambda = \infty$	6.335988×10^4
$\gamma(-2\omega; \omega, \omega, 0)$	$\lambda=1064$	8.257221×10^4
	$\lambda=1341$	7.497657×10^4
	$\lambda=1906$	6.927832×10^4

Table S6. Static and dynamic first hyperpolarizability (au) and depolarization ratio (DR) for $^{M@b_{64}/66}Al_{12}N_{12}$ (M= Sc- Zn) calculated by the sum-over-states method

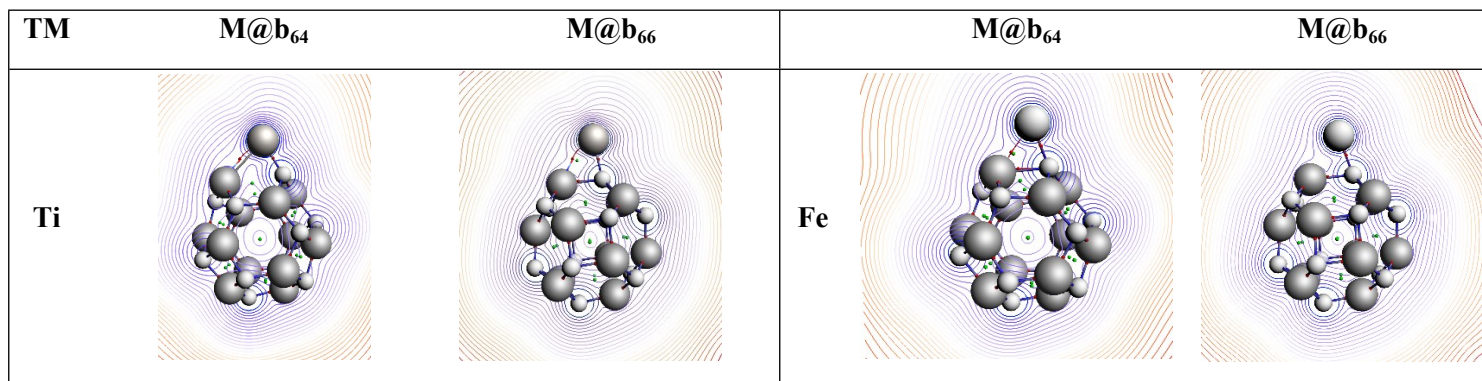
M@b ₆₄ Al ₁₂ N ₁₂	DR _{SOS} ^{$\lambda=\infty$}	$\beta_{SOS}^{\lambda=\infty}$	DR _{SOS} ^{$\lambda=1064$}	$\beta_{SOS}^{\lambda=1064}$	$\beta_{HRS,SOS}^{\lambda=1064}$	DR _{SOS} ^{$\lambda=1341$}	$\beta_{SOS}^{\lambda=1341}$	$\beta_{HRS,SOS}^{\lambda=1341}$	DR _{SOS} ^{$\lambda=1906$}	$\beta_{SOS}^{\lambda=1906}$	$\beta_{HRS,SOS}^{\lambda=1906}$
Sc	7.95	7169	3.39	579762.42	254237.97	3.77	25158.28	11935.39	2.91	25910.15	11545.39
Ti	7.57	2705	1.26	5615.41	4934.89	9.04	8127.36	6420.25	2.23	50405.91	24799.03
V	7.08	1677	2.29	32777.03	17301.48	5.24	9602.01	3848.64	8.11	6064.56	2288.99
Cr	6.63	2482	2.51	9460.03	4564.17	2.58	136959.32	57986.40	5.26	10129.52	3998.01
Mn	6.00	2225	4.23	44516.06	17989.43	7.06	15525.84	6215.46	5.46	15765.60	6287.04
Fe	4.95	1861	2.53	100581.62	43999.02	2.70	13131.09	5623.80	8.46	357206.52	296872.55
Co	5.07	1049	4.21	38457.14	15169.58	1.70	521762.19	244368.38	4.77	4471.14	1932.44
Ni	4.52	921	3.00	25495.52	10581.42	1.85	65945.66	29236.42	4.51	3325.50	1440.67
Cu	4.36	772	3.00	25131.65	10283.45	3.60E	9422.90	4051.41	4.21	3003.85	1305.23
Zn	3.32	696	3.17	3858.29	1792.65	3.32	2480.44	1165.14	3.34	1826.75	873.24

M@b₆₆Al₁₂N₁₂	$DR_{SOS}^{\lambda = \infty}$	$\beta_{SOS}^{\lambda = \infty}$	$DR_{SOS}^{\lambda = 1064}$	$\beta_{SOS}^{\lambda = 1064}$	$\beta_{HRS,SOS}^{\lambda = 1064}$	$DR_{SOS}^{\lambda = 1341}$	$\beta_{SOS}^{\lambda = 1341}$	$\beta_{HRS,SOS}^{\lambda = 1341}$	$DR_{SOS}^{\lambda = 1906}$	$\beta_{SOS}^{\lambda = 1906}$	$\beta_{HRS,SOS}^{\lambda = 1906}$
Sc	7.87	6899	1.99	895675.94	429355.59	1.95	100867.76	55537.23	2.56	13434.65	6274.06
Ti	7.70	5076	3.48	1249970.54	534462.42	4.39	143939.35	56509.46	6.91	21802.09	8663.13
V	7.46	2861	5.42	57731.03	24521.52	0.381	16862.81	20891.26	6.06	8546.79	3261.79
Cr	7.21	2484	1.59	12078.97	6555.81	2.25	72657.45	31325.23	5.80	10999.14	4227.26
Mn	6.14	2300	3.16	223110.52	93353.11	5.71	15095.19	6004.87	5.61	16605.87	6611.32
Fe	5.47	1853	2.70	83657.01	35652.31	2.90	12622.29	5415.79	5.80	10788.63	4505.63
Co	5.11	1398	2.92	68371.19	28797.71	1.42	8395.61	3905.82	5.42	6431.38	2763.05
Ni	4.24	852	2.96	42823.59	17857.47	1.91	21322.15	10293.98	4.54	3452.04	1520.84
Cu	4.20	672	2.86	33042.36	13688.67	3.21	16463.31	7098.13	4.15	3001.29	1318.85
Zn	2.61	558	2.64	3307.94	1618.21	2.75	1913.48	973.17	2.69	1314.08	703.96



$M@b_{64}Al_{12}N_{12}$ $M@b_{66}Al_{12}N_{12}$

Scheme S1. Optimized geometry of the title compounds



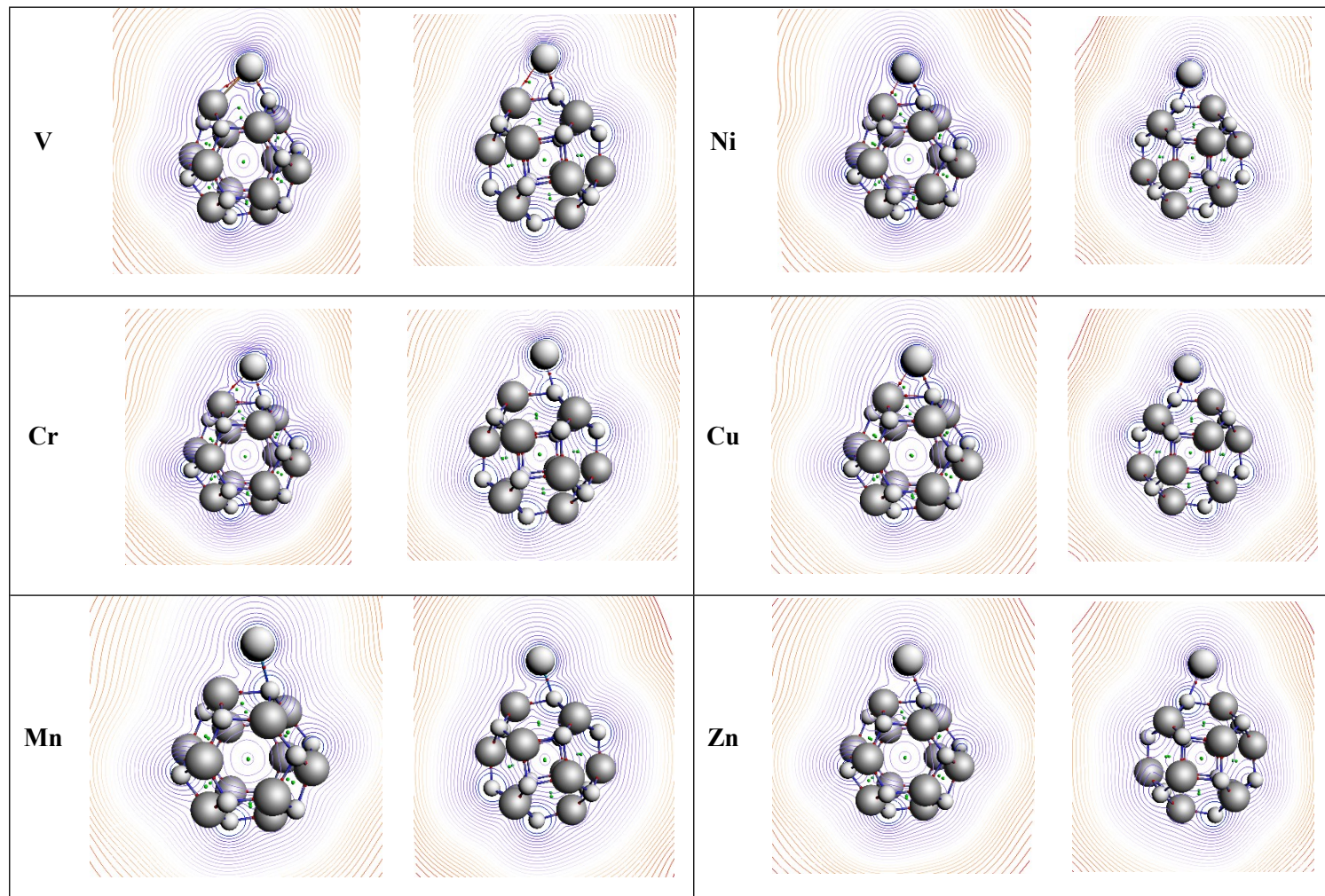
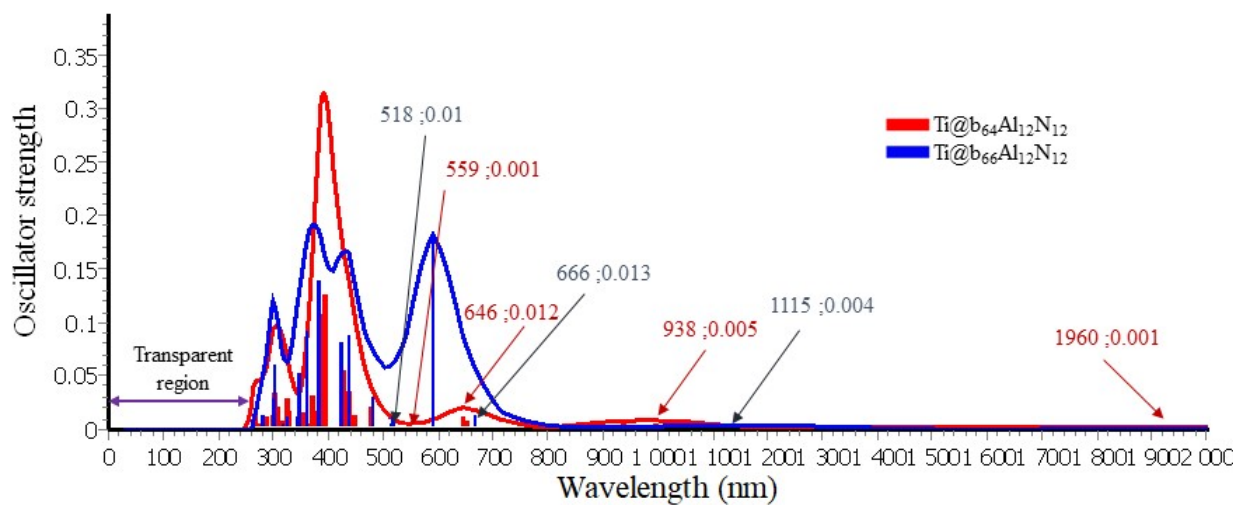
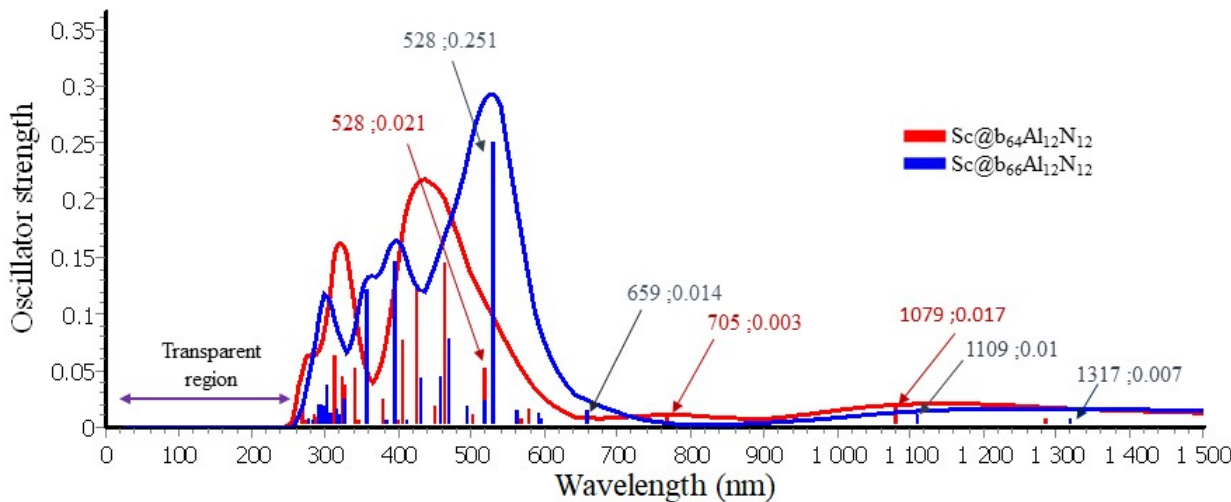
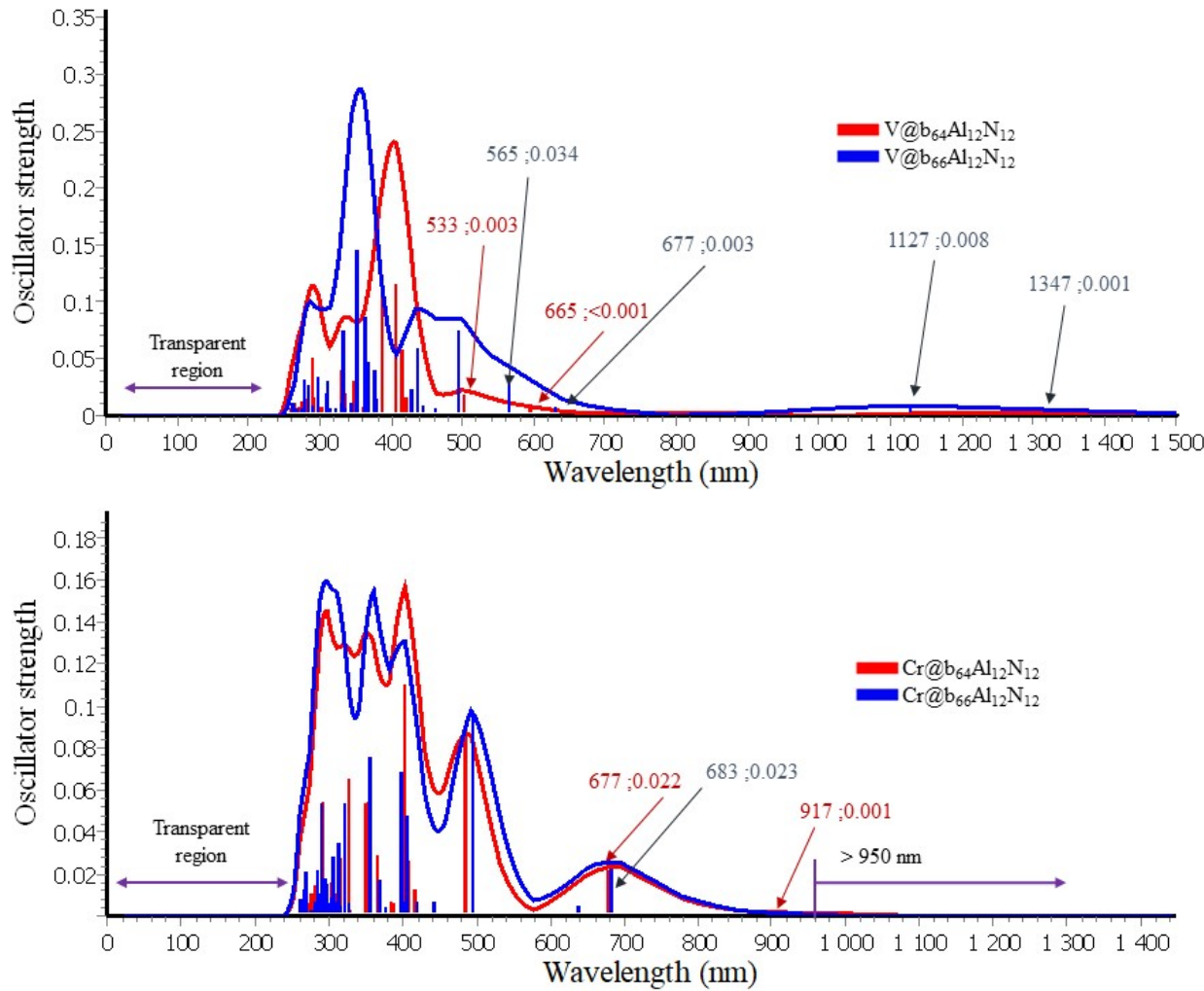
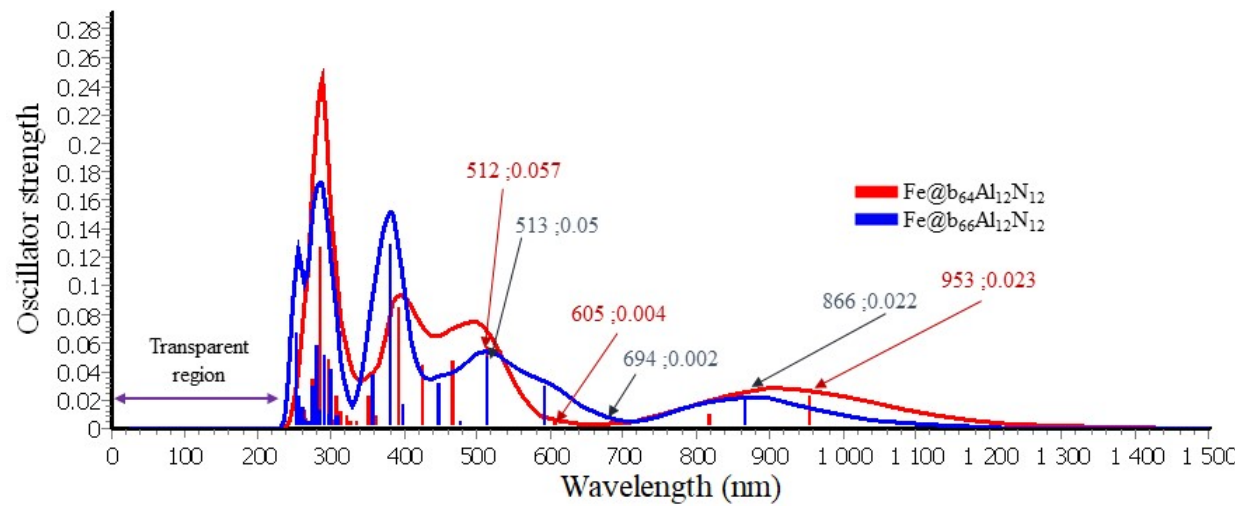
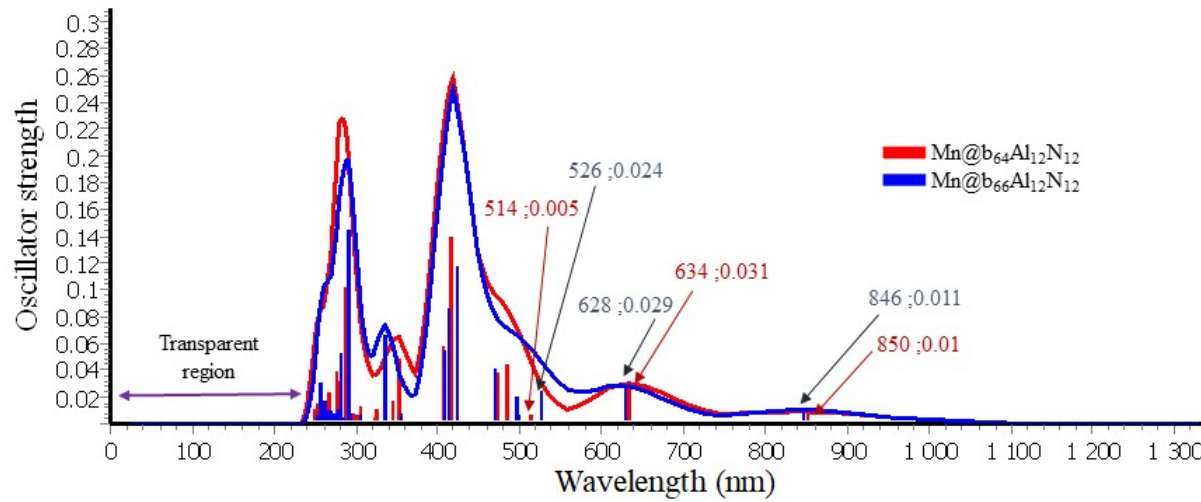
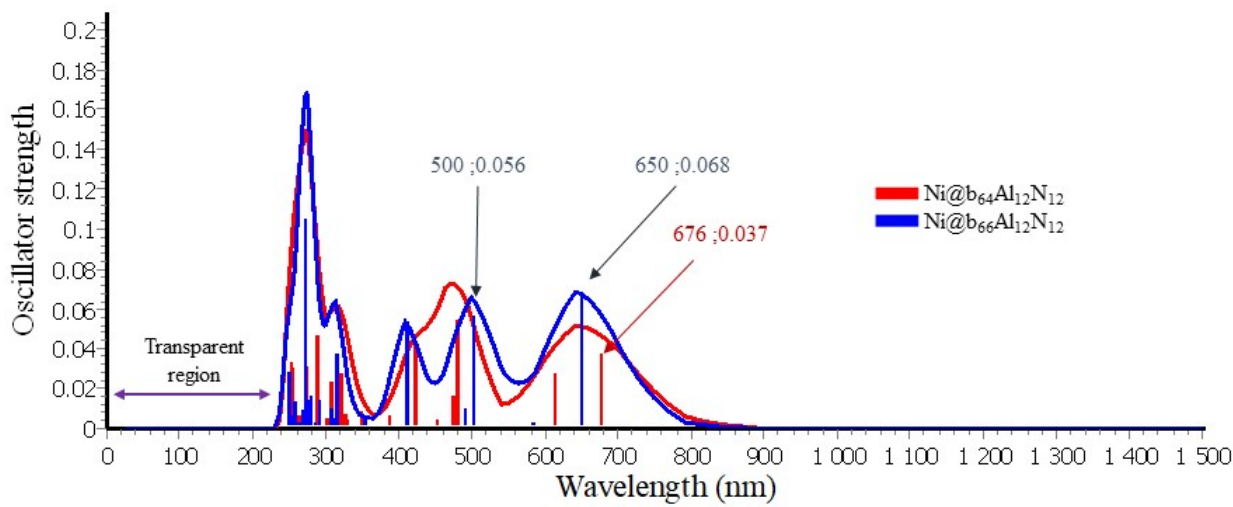
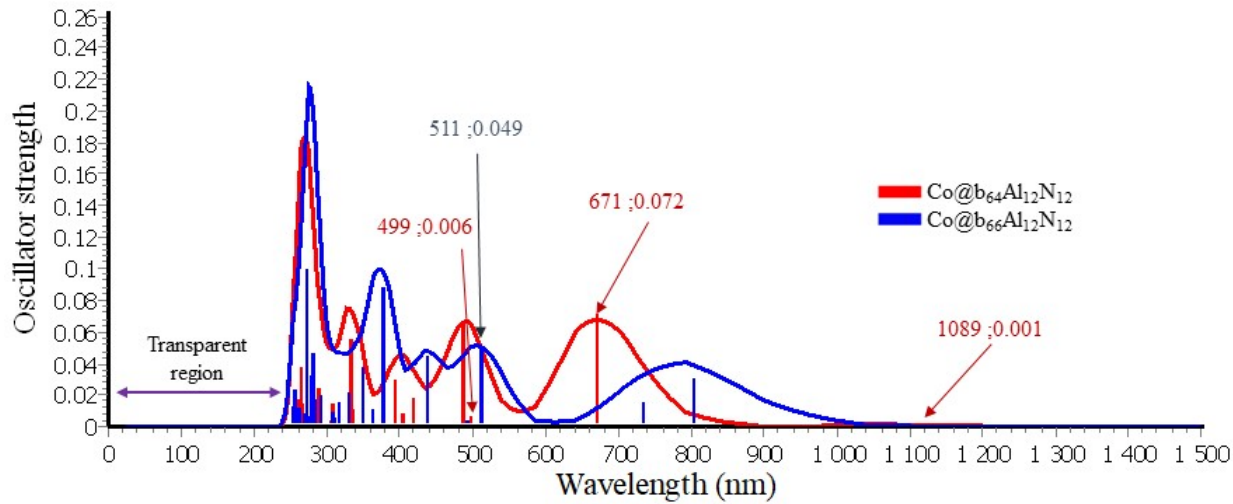


Figure S1. Molecular topology of $M@b_{64/66}Al_{12}N_{12}$ ($M = Sc-Zn$) where in the nanocage, nitrogen atoms: are small spheres, while aluminum atoms: are large spheres.









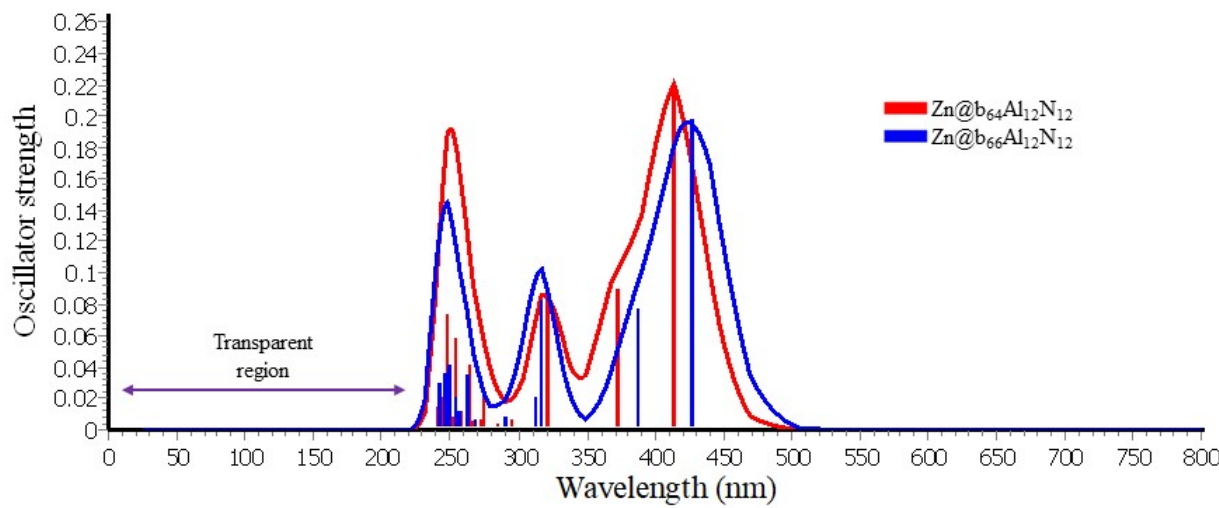
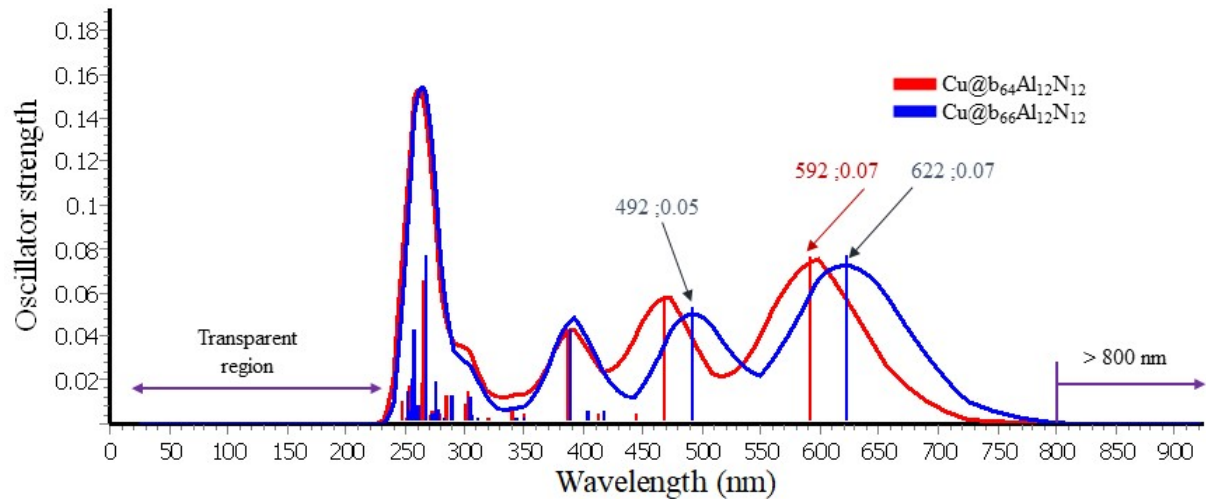
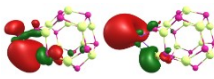
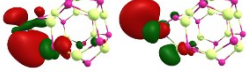
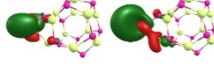
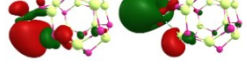
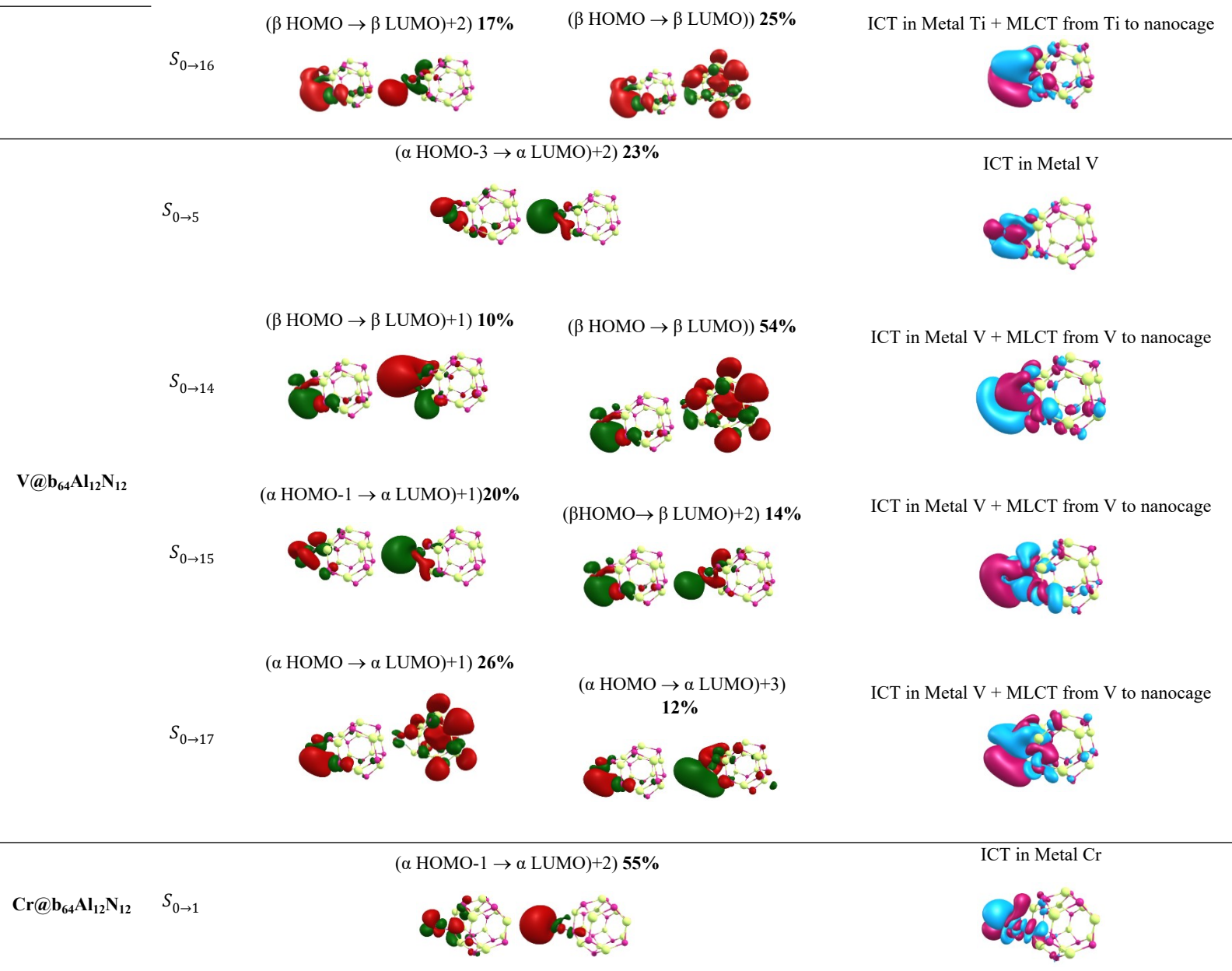
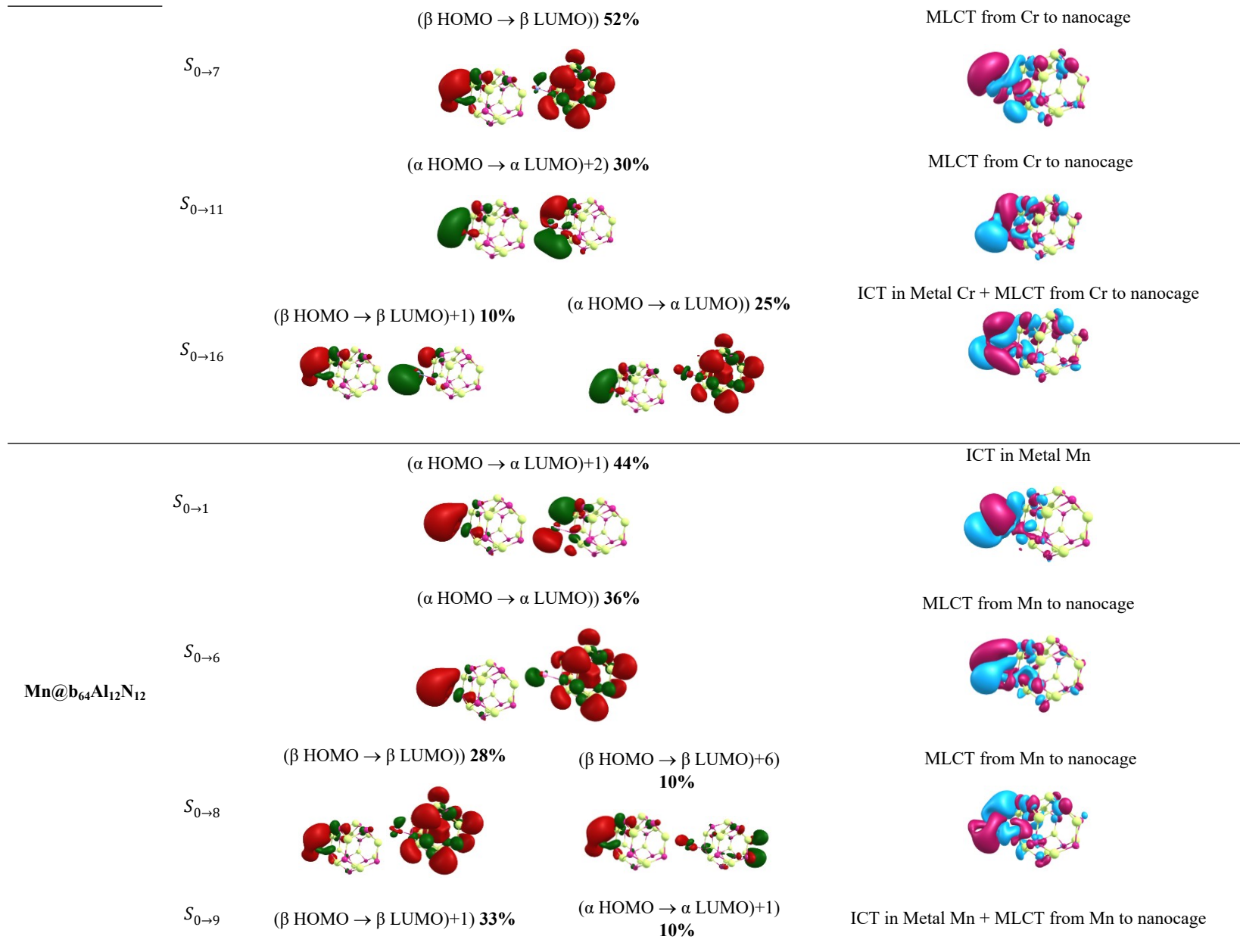
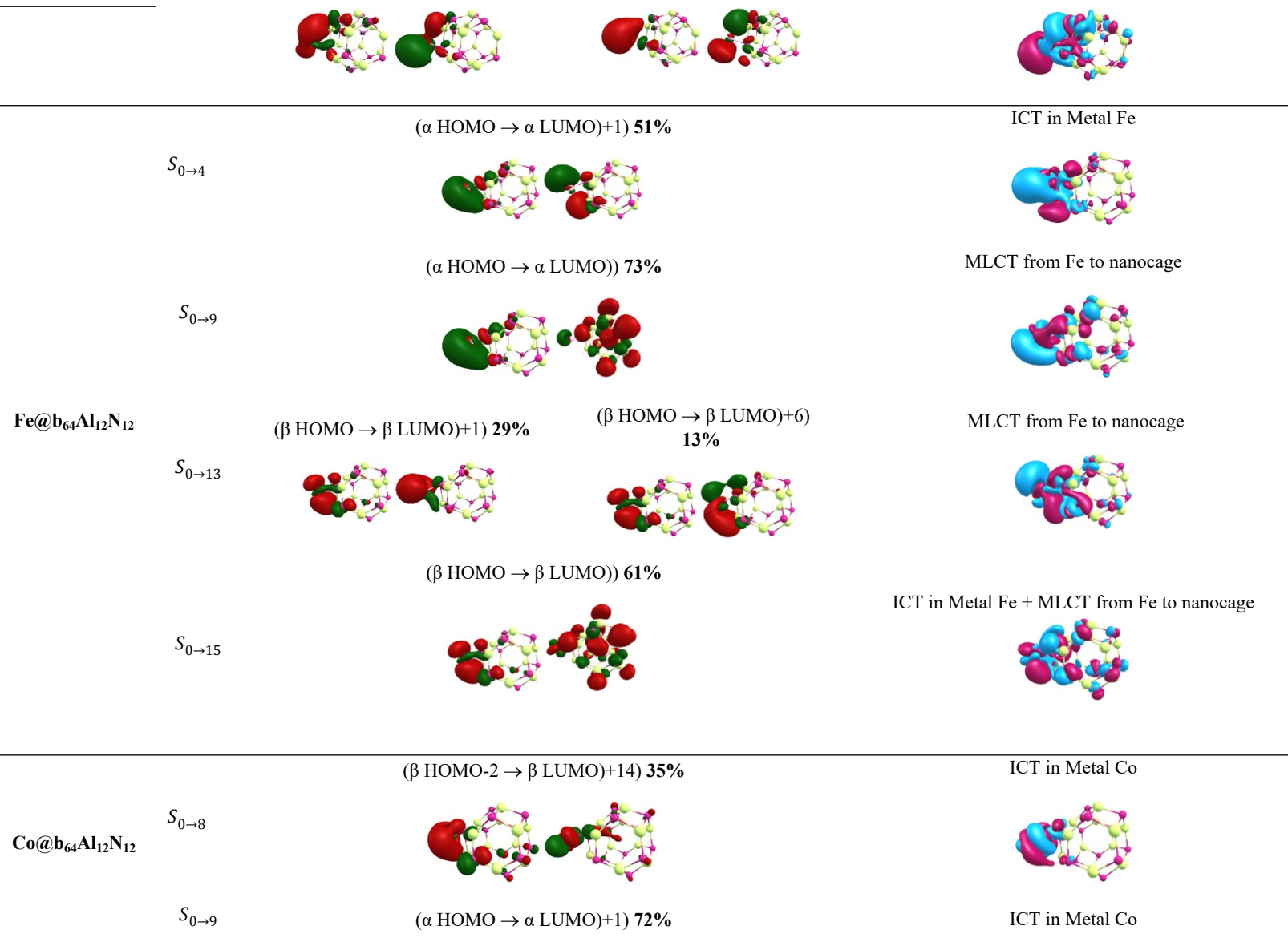


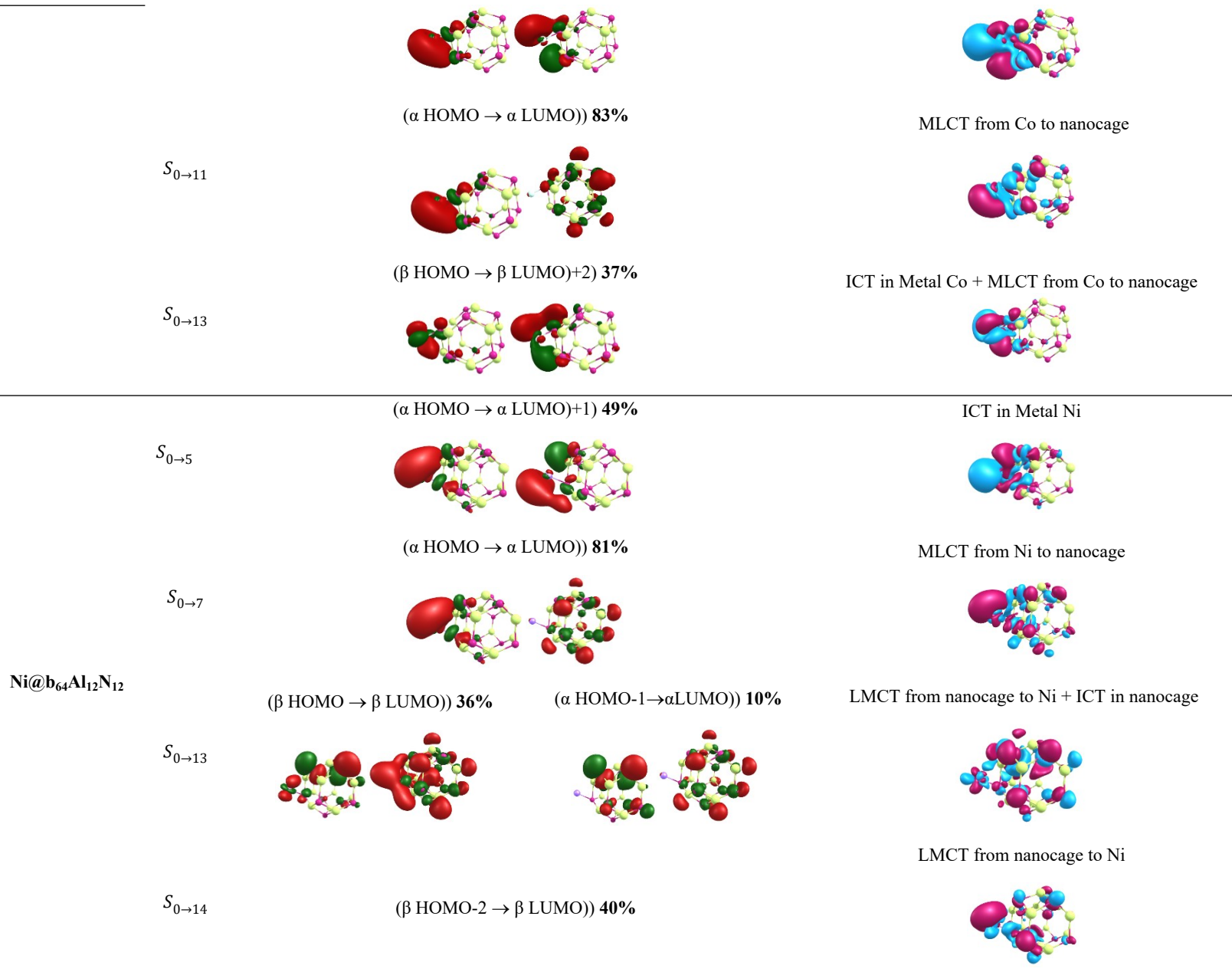
Figure S2. Calculated UV – vis absorption spectra of $M@\text{b}_{64/66}\text{Al}_{12}\text{N}_{12}$ (M from Sr to Zn)

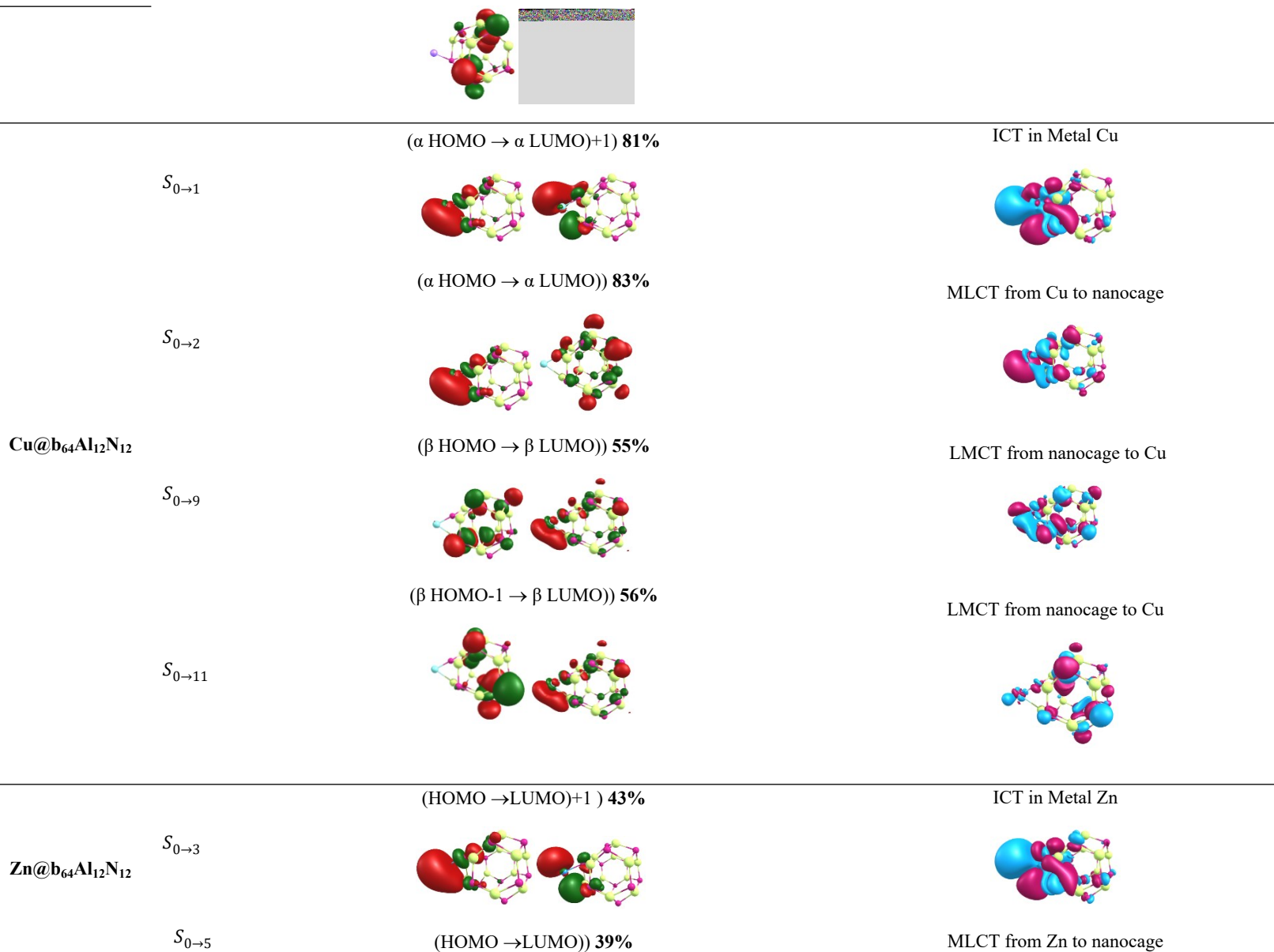
M@b₆₄Al₁₂N₁₂	$S_{0 \rightarrow n}$	MO	(EDDM)
		(β HOMO → β LUMO) 49 %	ICT in Metal Sc
	$S_{0 \rightarrow 5}$		
		(βHOMO → βLUMO)+4) 10%	ICT in Metal Sc + MLCT from Sc to nanocage
	$S_{0 \rightarrow 11}$		
Sc@b₆₄Al₁₂N₁₂		(α HOMO-1 → α LUMO)+1) 15%	ICT in Metal Sc + MLCT from Sc to nanocage
	$S_{0 \rightarrow 13}$		
		(β HOMO → β LUMO)+2) 18%	ICT in Metal Sc + MLCT from Sc to nanocage
	$S_{0 \rightarrow 15}$		
		(α HOMO → α LUMO)+1) 22%	ICT in Metal Ti
	$S_{0 \rightarrow 5}$		
		(β HOMO → β LUMO)+1) 10%	ICT in Metal Ti + MLCT from Ti to nanocage
Ti@b₆₄Al₁₂N₁₂	$S_{0 \rightarrow 15}$		
		(α HOMO-2 → α LUMO)+3) 13%	ICT in Metal Ti + MLCT from Ti to nanocage
	$S_{0 \rightarrow 18}$		



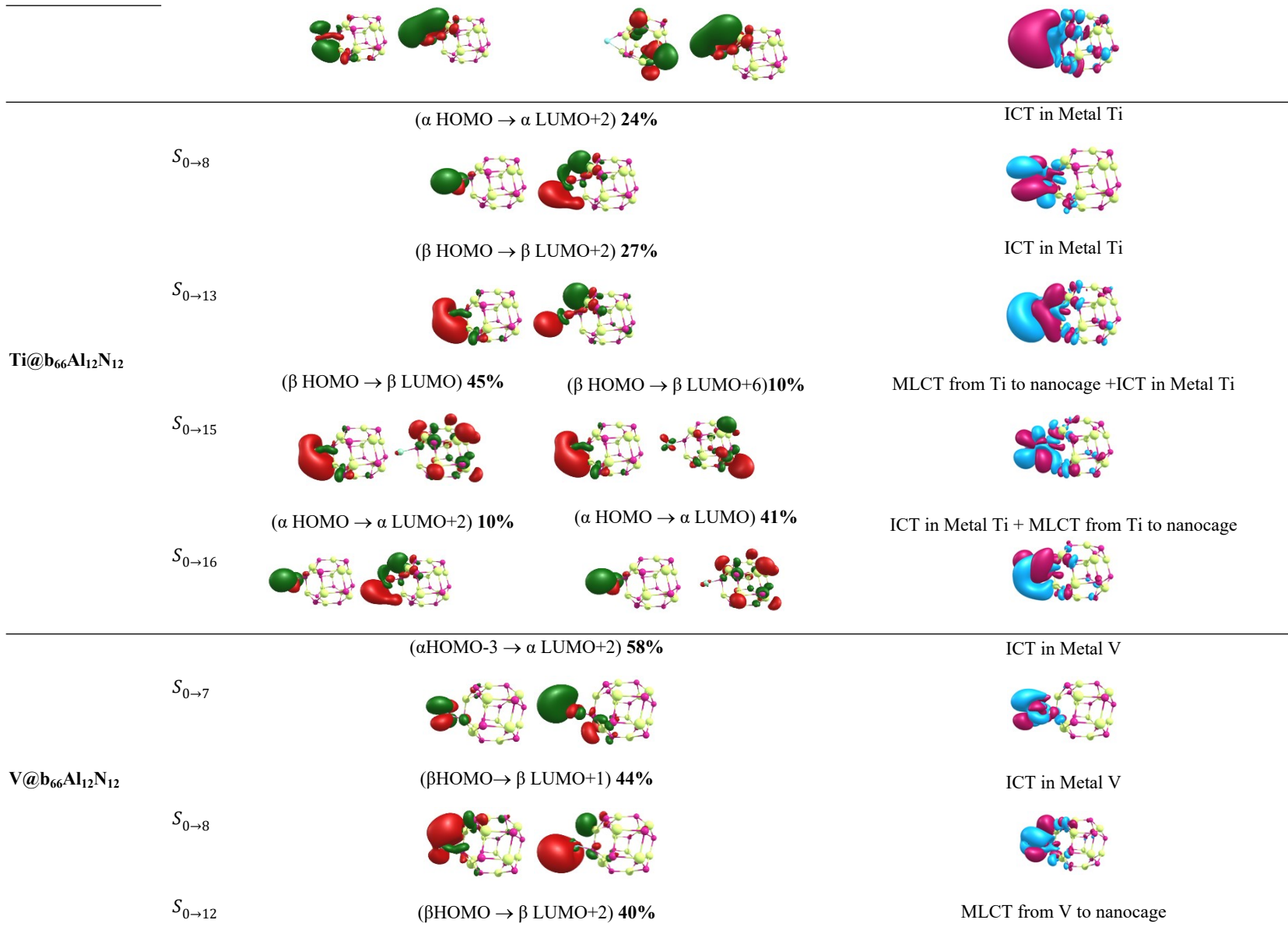


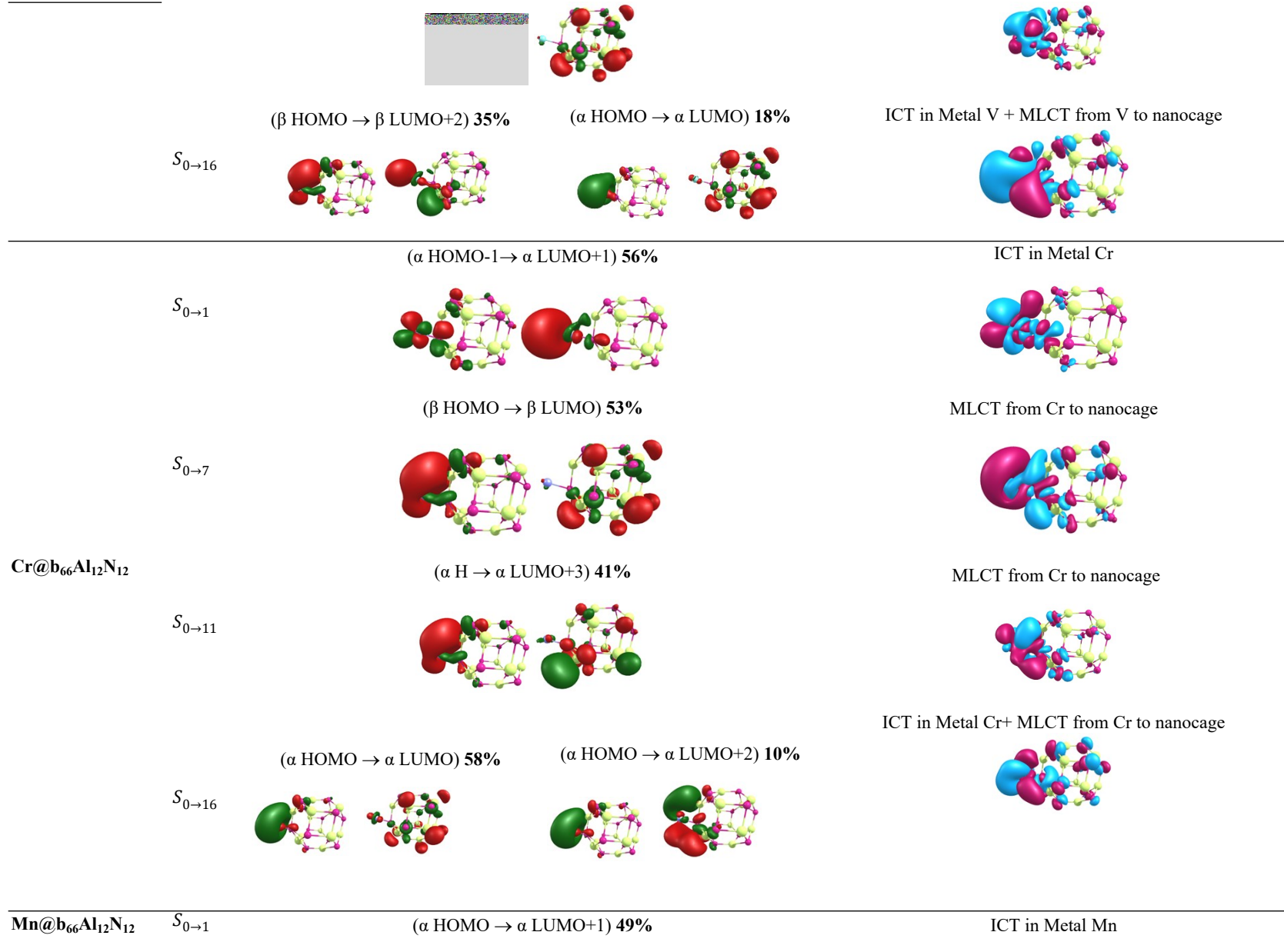


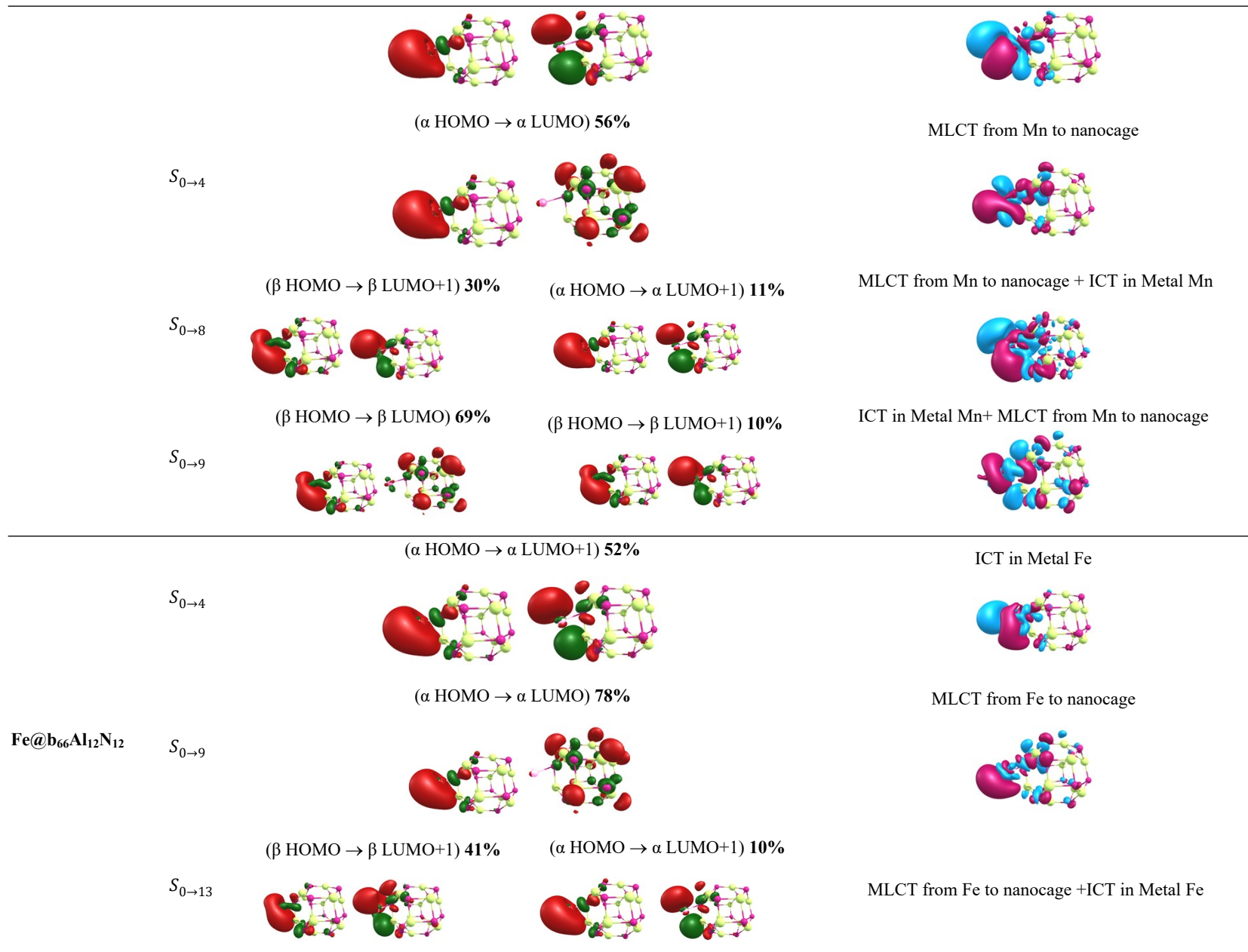


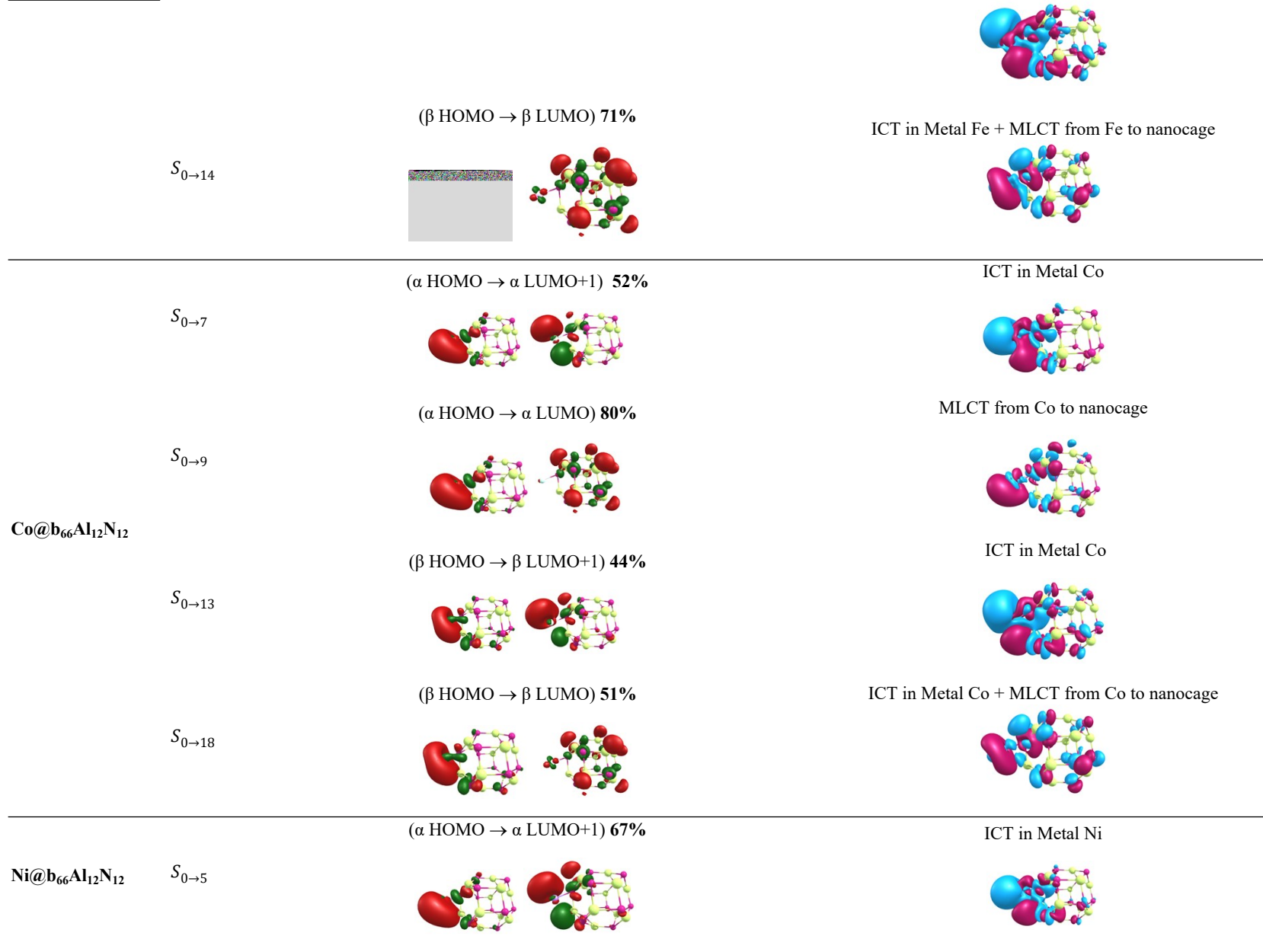


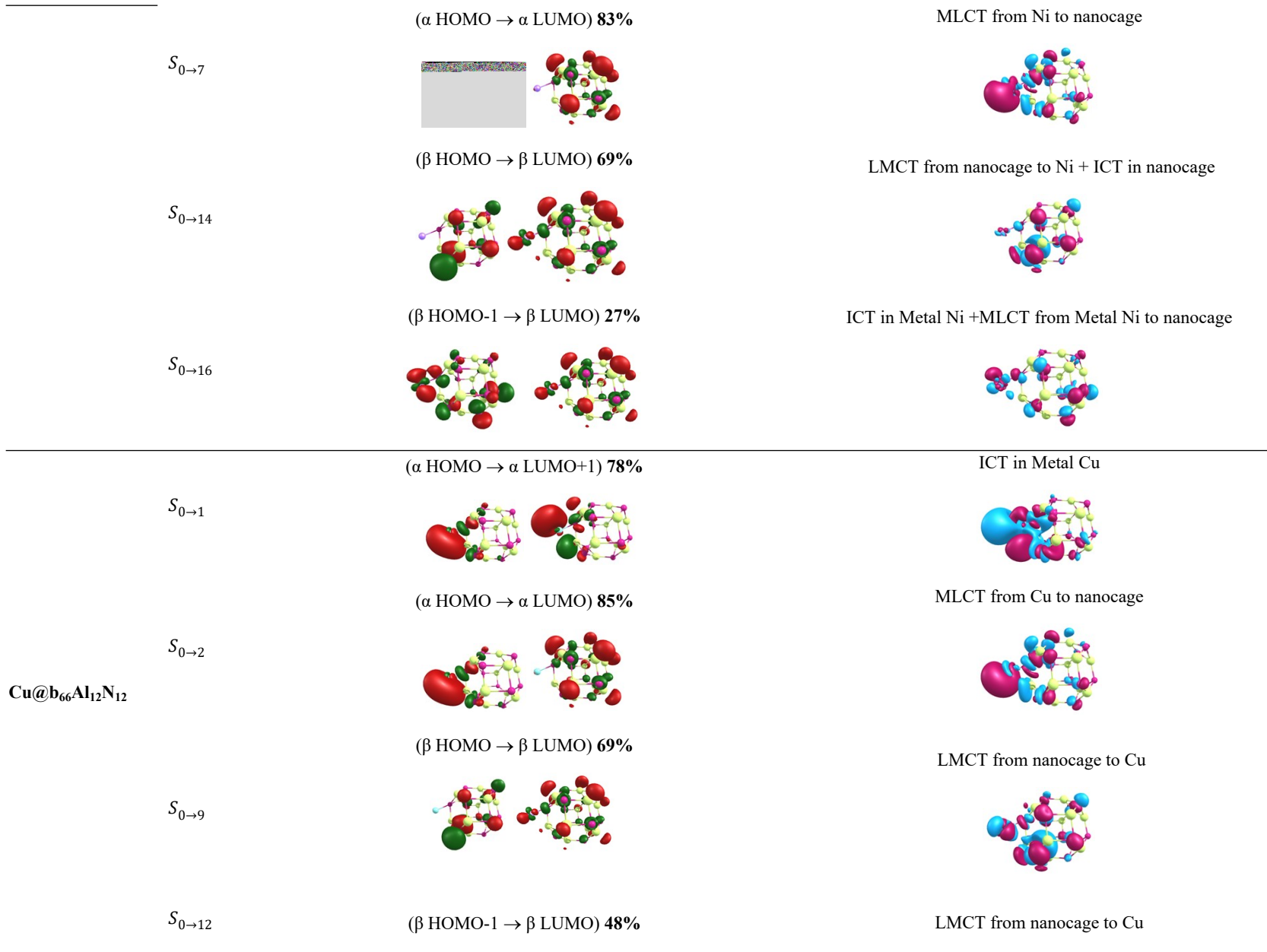
		(HOMO → LUMO)+2) 37%	MLCT from Zn to nanocage
$S_{0 \rightarrow 8}$			ICT in nanocage + LMCT from nanocage to Zn
$S_{0 \rightarrow 11}$			EDDM
M@b₆₆Al₁₂N₁₂	$S_{0 \rightarrow n}$	MO	
		(α HOMO → α LUMO+1) 30%	ICT in Metal Sc
$S_{0 \rightarrow 6}$			MLCT from Sc to nanocage
$S_{0 \rightarrow 10}$			ICT in Metal Sc + MLCT from Sc to nanocage
$S_{0 \rightarrow 13}$			ICT in Metal Sc + LMCT from nanocage to Sc
$S_{0 \rightarrow 24}$	(α HOMO-1 → α LUMO+3) 19% (β HOMO → β LUMO+2) 21%		











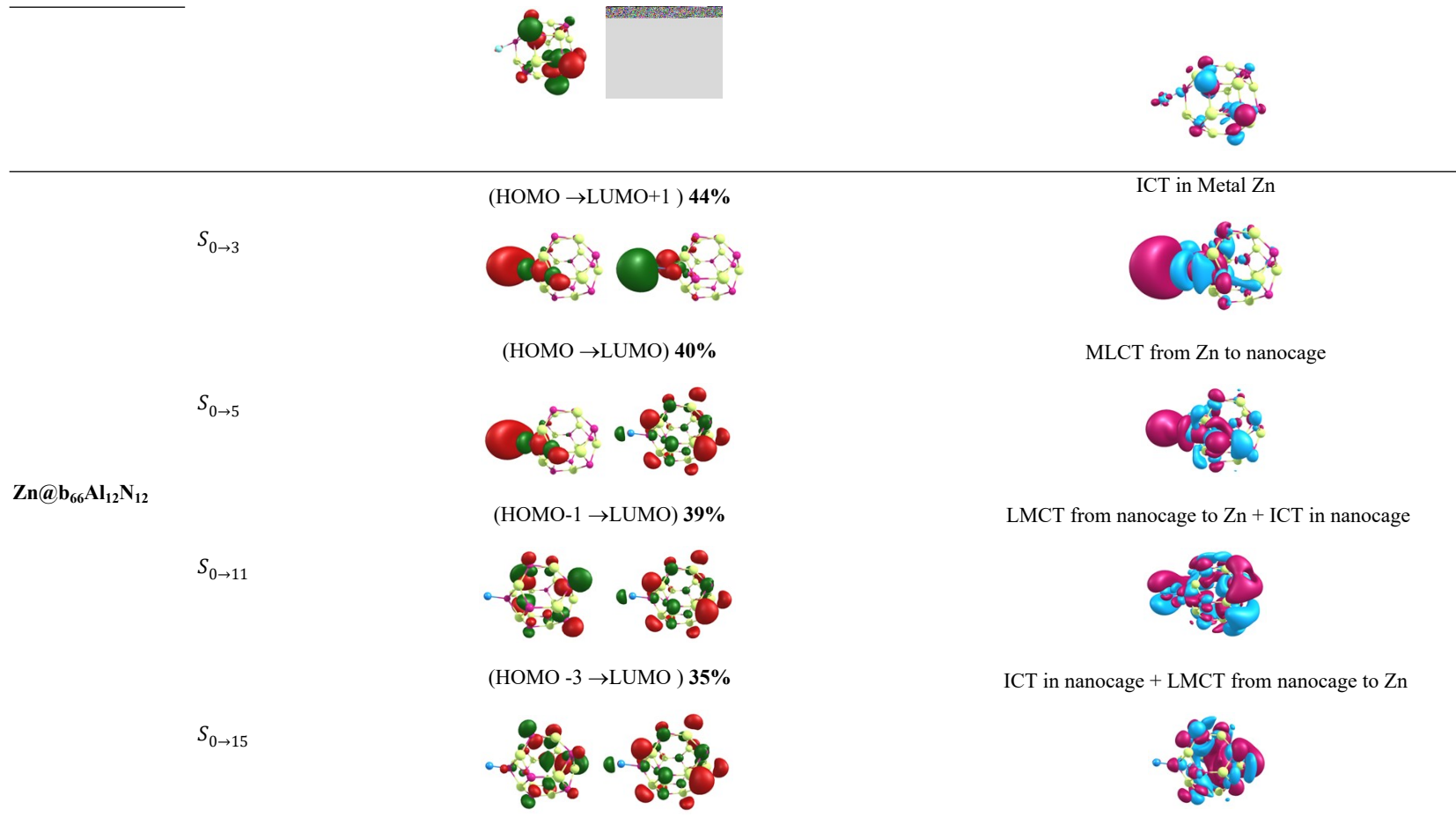


Figure S3. Molecular orbitals (MO) and electron density difference maps (EDDM) for the crucial excited states of $\mathbf{M}@\mathbf{b}_{64}\mathbf{Al}_{12}\mathbf{N}_{12}$ and $\mathbf{M}@\mathbf{b}_{66}\mathbf{Al}_{12}\mathbf{N}_{12}$

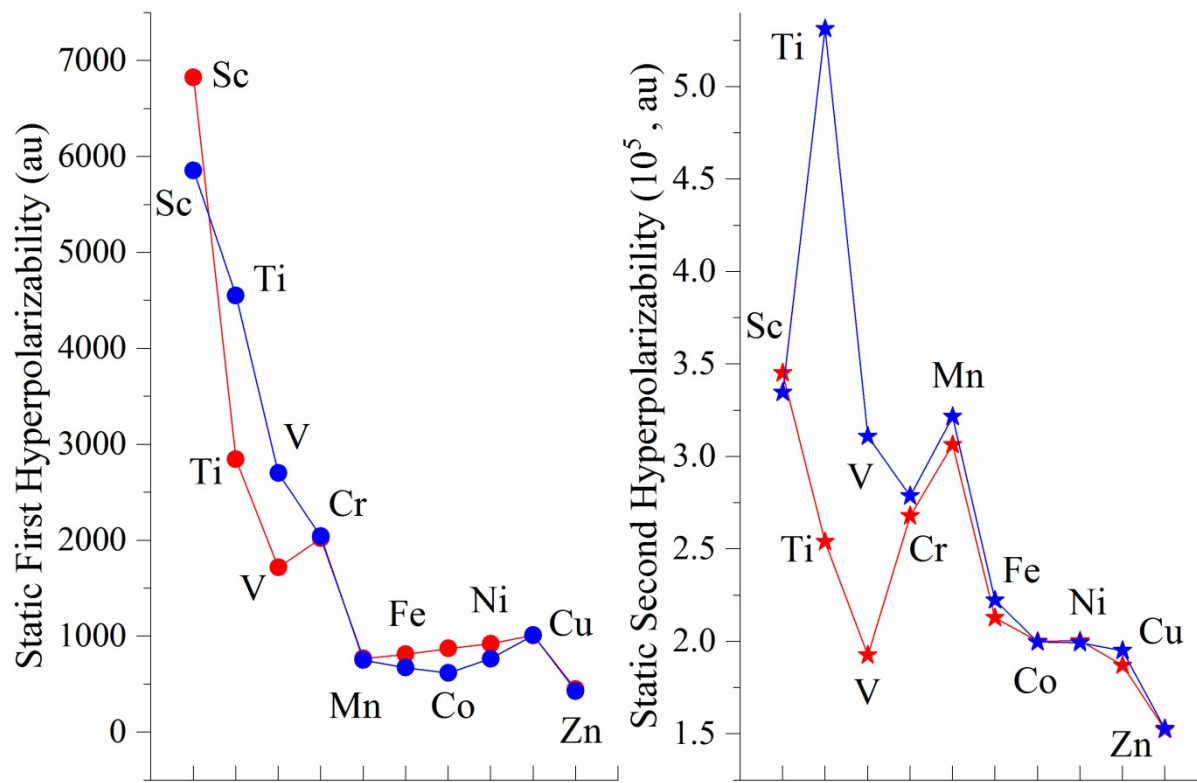
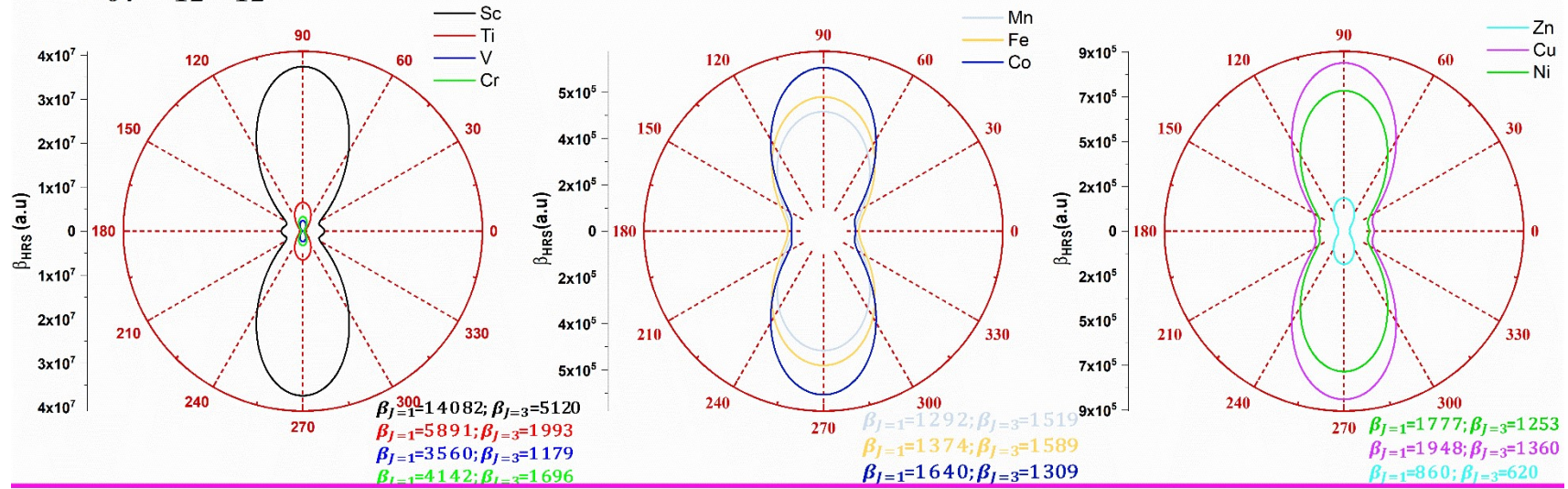


Figure S4. Variation of first hyperpolarizability (β_{HRS}^∞) and second hyperpolarizability ($\gamma(0;0,0,0)$) of $M@b_{64}Al_{12}N_{12}$ (red) and $M@b_{66}Al_{12}N_{12}$ (blue) where M= Sc-Zn

M@b₆₄Al₁₂N₁₂



M@b₆₆Al₁₂N₁₂

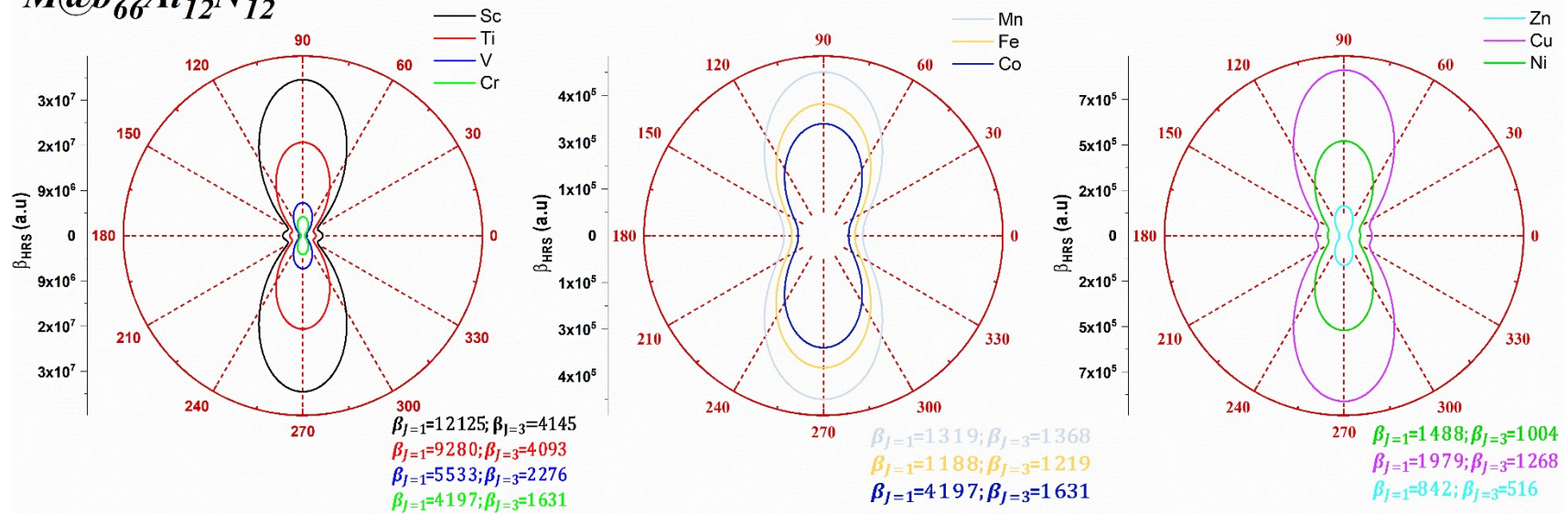


Figure S5. Relationship between I_{Ψ}^{2w} and polarization angle Ψ of $M@b_{64/66}Al_{12}N_{12}$

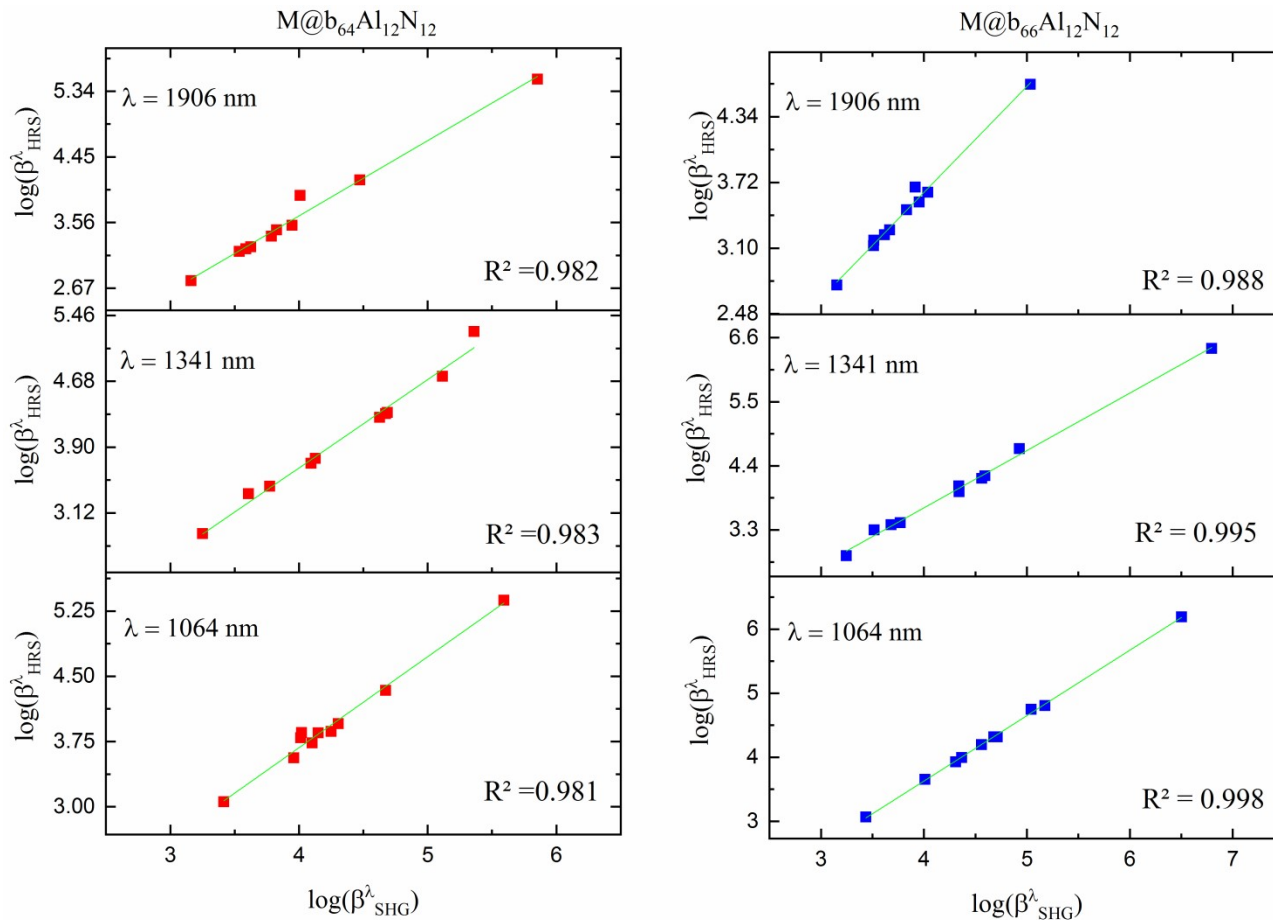


Figure S6. Plot of β_{HRS}^λ as a function of β_{SHG}^λ for $M@b_{64/66}Al_{12}N_{12}$, where $M = \text{Sc to Zn}$, 1906, 1341, and 1064 nm